

AWARD NUMBER: W81XWH-13-1-0317

TITLE: A Computational Framework for Design and Development of
Novel Prostate Cancer Therapies

PRINCIPAL INVESTIGATOR: Gaurav Bhardwaj

CONTRACTING ORGANIZATION: University of California, Davis
Davis, CA 95618

REPORT DATE: September 2015

TYPE OF REPORT: Annual

PREPARED FOR: U.S. Army Medical Research and Materiel Command
Fort Detrick, Maryland 21702-5012

DISTRIBUTION STATEMENT: Approved for Public Release;
Distribution Unlimited

The views, opinions and/or findings contained in this report are those of the author(s) and should not be construed as an official Department of the Army position, policy or decision unless so designated by other documentation.

REPORT DOCUMENTATION PAGE				Form Approved OMB No. 0704-0188	
Public reporting burden for this collection of information is estimated to average 1 hour per response, including the time for reviewing instructions, searching existing data sources, gathering and maintaining the data needed, and completing and reviewing this collection of information. Send comments regarding this burden estimate or any other aspect of this collection of information, including suggestions for reducing this burden to Department of Defense, Washington Headquarters Services, Directorate for Information Operations and Reports (0704-0188), 1215 Jefferson Davis Highway, Suite 1204, Arlington, VA 22202-4302. Respondents should be aware that notwithstanding any other provision of law, no person shall be subject to any penalty for failing to comply with a collection of information if it does not display a currently valid OMB control number. PLEASE DO NOT RETURN YOUR FORM TO THE ABOVE ADDRESS.					
1. REPORT DATE September 2015		2. REPORT TYPE Annual		3. DATES COVERED 1 Sep 2014 - 31 Aug 2015	
4. TITLE AND SUBTITLE A Computational Framework for Design and Development of Novel Prostate Cancer Therapies				5a. CONTRACT NUMBER	
				5b. GRANT NUMBER W81XWH-13-1-0317	
				5c. PROGRAM ELEMENT NUMBER	
6. AUTHOR(S) Gaurav Bhardwaj E-Mail:gauravcd34@gmail.com				5d. PROJECT NUMBER	
				5e. TASK NUMBER	
				5f. WORK UNIT NUMBER	
7. PERFORMING ORGANIZATION NAME(S) AND ADDRESS(ES) UNIVERSITY OF CALIFORNIA, DAVIS 1850 RESEARCH PARK DR, STE 300 DAVIS CA 95618-6134				8. PERFORMING ORGANIZATION REPORT NUMBER	
9. SPONSORING / MONITORING AGENCY NAME(S) AND ADDRESS(ES) U.S. Army Medical Research and Materiel Command Fort Detrick, Maryland 21702-5012				10. SPONSOR/MONITOR'S ACRONYM(S)	
				11. SPONSOR/MONITOR'S REPORT NUMBER(S)	
12. DISTRIBUTION / AVAILABILITY STATEMENT Approved for Public Release; Distribution Unlimited					
13. SUPPLEMENTARY NOTES					
14. ABSTRACT Tek protein kinases, such as Etk and Btk, play key roles in the survival and proliferation of prostate cancer cells. We developed novel computational and combinatorial frameworks for design and development of small molecule inhibitors targeting Etk. Large scale <i>in silico</i> screening of virtual libraries was used to identify novel Etk inhibitors. Experimental studies with small-molecule ligands identified from computational screens show promising cell growth inhibition for PC3 cells in cell culture based experiments. In addition, we used phylogenetic and structural studies to identify novel target sites. Overall, the computational methods developed here can be used to rapidly scan and develop potent enzyme inhibitors, and more generally provide drug leads for late-stage prostate cancer.					
15. SUBJECT TERMS Computational Drug Design, Tyrosine kinase Inhibitors, Late-stage Prostate Cancer					
16. SECURITY CLASSIFICATION OF:			17. LIMITATION OF ABSTRACT Unclassified	18. NUMBER OF PAGES 26	19a. NAME OF RESPONSIBLE PERSON USAMRMC
a. REPORT Unclassified	b. ABSTRACT Unclassified	c. THIS PAGE Unclassified			19b. TELEPHONE NUMBER (include area code)

Table of Contents

	<u>Page</u>
1. Introduction.....	2
2. Keywords.....	2
3. Overall Project Summary.....	2
4. Key Research Accomplishments.....	9
5. Conclusion.....	10
6. Publications, Abstracts and Presentations.....	10
7. Inventions, Patents and Licenses.....	11
8. Reportable Outcomes.....	11
9. Training Program.....	11
10. References.....	12
11. Appendices.....	14

INTRODUCTION

Prostate Cancer (CaP) continues to be a significant health and mortality risk among men. Effective therapies that target late stages of CaP are largely lacking, and need development. Research efforts by our group and others, have previously established that signaling pathways mediated by non-receptor tyrosine kinases, such as Etk, Btk and Src kinase, impart strong survival signals and capabilities to prostate cancer cells¹⁻⁶. We had originally proposed to use computational and combinatorial methods to develop potent and effective inhibitors against these Tek kinases. Over the period of this grant, we have (i) **developed novel computational tools** and pipelines for complementing the large scale combinatorial approaches, (ii) used computational tools to explain the **mode of action for novel inhibitors of Tek kinases** identified in these screens, and (iii) computationally designed **multiple new inhibitors** with good potency. Further, we have conducted multiple sequence-based, and structure-based comparative studies of the Tec-family of kinases (Tek), to **identify novel target sites**; and design strategies for targeting these sites along with our primary target of kinase active site.

KEYWORDS

Tek kinase inhibitors, Late-stage Prostate Cancer Therapy, Castration Resistant Prostate Cancers, Rational Drug Design, Computational Design, Small-molecule ligands, Combinatorial Drug Design

OVERALL PROJECT SUMMARY

During the period of this grant, we have made significant progress on using computational and combinatorial methods for designing, synthesizing and validating multiple lead compounds that target Tek kinases, such as Btk, Itk and Etk. We have also developed new computational tools and pipelines for designing small-molecule, as well as peptide inhibitors for the Tek kinases.

Note about the grant transfer and funding status

Following the last annual report, PI Gaurav Bhardwaj had to move from University of California, Davis, to University of Washington, Seattle. The grant has remained in “pending transfer” status since then (>15 months), and has not been actively funded in the last funding period. However, I have continued to make some progress on developing computational tools for designing peptide-based inhibitors of Tek kinases, as well as the training goals proposed in the original proposal. In this update, I summarise that work, along with the work done by me so far on the development of small molecule inhibitors targeting Tek kinases.

Specific Aim 1: Designing and Screening Theoretical *in silico* drug libraries

We have developed new computational pipelines to develop virtual small-molecule libraries, and used *in silico* screening to identify new lead compounds that inhibit members of Tek kinase family.

Task 1a: Primary Virtual Screen of Small Molecule Libraries with Autodock

First, we sought to decipher the modes of binding and inhibition for the Tek inhibitors identified from our combinatorial screens. Specifically, we identified CTN06, a dual inhibitor of Btk and Etk⁷; and CTN095⁸, a dual inhibitor of Etk and Src kinase (Figure 1). It was essential to understand the binding site, and the mode of action for these inhibitors to further design a virtual library focused on improved binding affinity and inhibitory activity. Blind computational docking was used to globally scan the Tek kinase structures for most likely binding sites. Next, fine-grained docking studies were conducted using Autodock⁹ and Rosetta Ligand Docking¹⁰ in these putative binding sites to scan for the most likely binding-mode based on the computational binding energies for each docked pose. Lastly, molecular dynamics simulations were conducted starting from the docked conformations to validate the stability of the proposed binding mode¹¹.

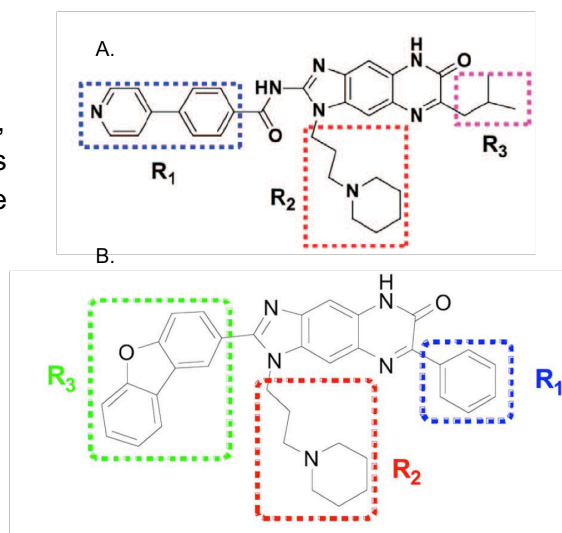


Figure1: Chemical Structure of (A) CTN06 (B) CTA095

Our *in silico* studies showed that CTN06 inhibits the kinase activity of Btk and Etk by binding to the the back-pocket of the ATP binding site, and interacting with the structural motifs essential for the active state conformation, such as the gatekeeper residue (T447) and the DFG loop (Figure 2). Importantly, the trends in theoretically calculated computational binding energies for CTN06 binding to Btk and Etk, recapitulate the differences in experimentally determined binding energies. This further proves that the computational pipeline is able to identify and distinguish between closely related binding modes with sufficient confidence. Similar studies conducted to explore the binding mode of CTA095 to Etk and Src kinase also showed that CTA095 interacts with the back-pocket and stabilizes these kinases in their inactive states upon binding (Figure 3). In addition to these compounds, we have also identified other small molecule ligands that inhibit related Tek kinase family members, such as Itk. The binding modes for these classes of inhibitors follow a similar trend: binding near the ATP binding pocket, and/or stabilizing the inactive conformation of these kinases.

Having identified the binding modes for CTA095 and CTN06, we used the structural and biochemical information of these binding modes and binding pockets, to direct the generation of virtual small molecule libraries. We designed several libraries diversifying the R₁, R₂, R₃, and the core scaffold of the CTN06 (CTX series) (Figure 4). Further, some virtual libraries (CTG series) (Figure 5) were also designed to have more linear shapes to provide better shape complementarity with the binding pockets. Large scale docking studies were conducted targeting Etk to screen for the small molecule compounds that provided better binding energies than our previously known compounds. Molecules that passed the initial docking filters were subjected to further *in silico* secondary screens.

Task 1b: Identification of Next generation of Tek Kinase inhibitors

Ligands that passed our initial docking screens using Autodock were further screened using Rosetta ligand docking methods¹⁰, and molecular dynamics. Comparative analysis of the

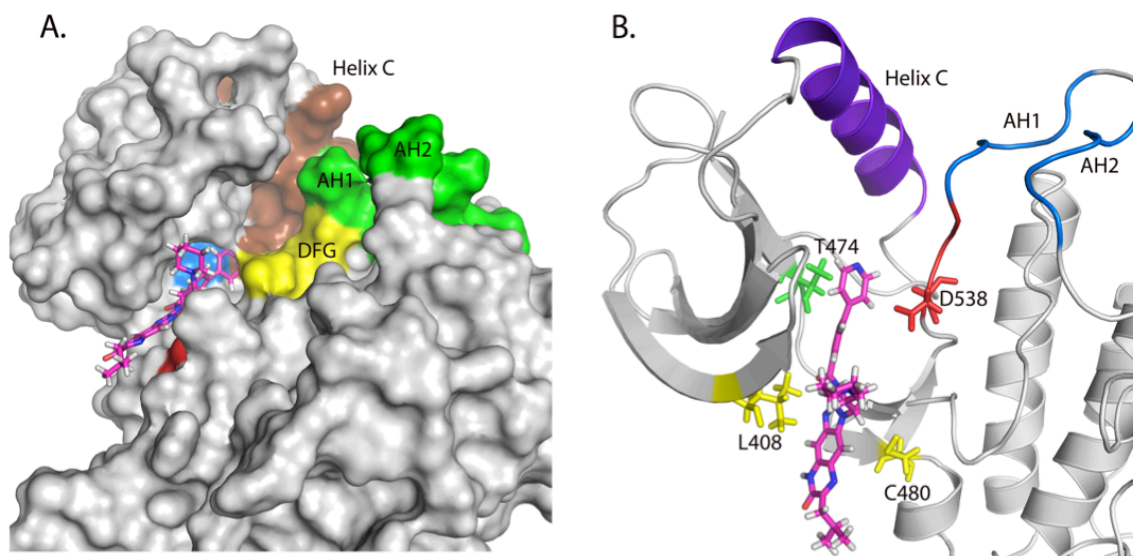


Figure2: Computational Docking of CTN06 to Btk. (A) Surface view of Btk docked to CTN06 after 20 ns of MD relaxation. Brown: helix C (439–452); green: activation loop helix 1 (AH1) (541–546) and activation loop helix 2 (AH2) (548–553); yellow: DFG motif (538–540); blue: Thr474; red: Cys480. (B) Cartoon representation showing predicted interactions of Btk with CTN06. Thr474, Leu408, Cys480 and Asp538 side chains are shown as sticks and colored based on residue type (red: acidic, green: polar, yellow: non-polar). DFG motif is shown in red. Figures were generated using PyMol

computational binding energies identified multiple compounds that displayed better binding energies than CTN06 and CTA095 (Table 1 and 2). Specifically, CTG06 and CTG02 show exceptional binding affinities, that surpass our previously established inhibitors. The linear nature of the CTG series library also provides for very good shape complementarity in the binding mode. Additionally, we have also identified compounds from the 3-pronged CTX library that provided better binding energies than CTA095. Molecular dynamics trajectories in explicit solvent conditions also confirmed that these new lead compounds bind in a stable manner to their target.

As we learnt from the phylogenetic and structural modeling in Specific Aim 2, there is very high structural similarities between different family members of the Tek kinase family. Given the general limitations associated with small molecule therapeutics, such as the lack of specificity, and off-target effects, we also decided to explore the possibility of **rationally designing peptide-based therapeutics targeting Tek kinases**. Peptide-based therapeutics based on stapled/constrained peptides can have exquisite specificity and selectivity due to their larger surface area, while still retaining the stabilities similar to the traditional small molecule drugs. However, structure-based approaches to design peptide-based therapeutics are currently limited by the lack of diversity among natural constrained peptides. We have focused our efforts on developing computational methods that can design constrained peptides across diverse topologies with precise control over their shape and size.

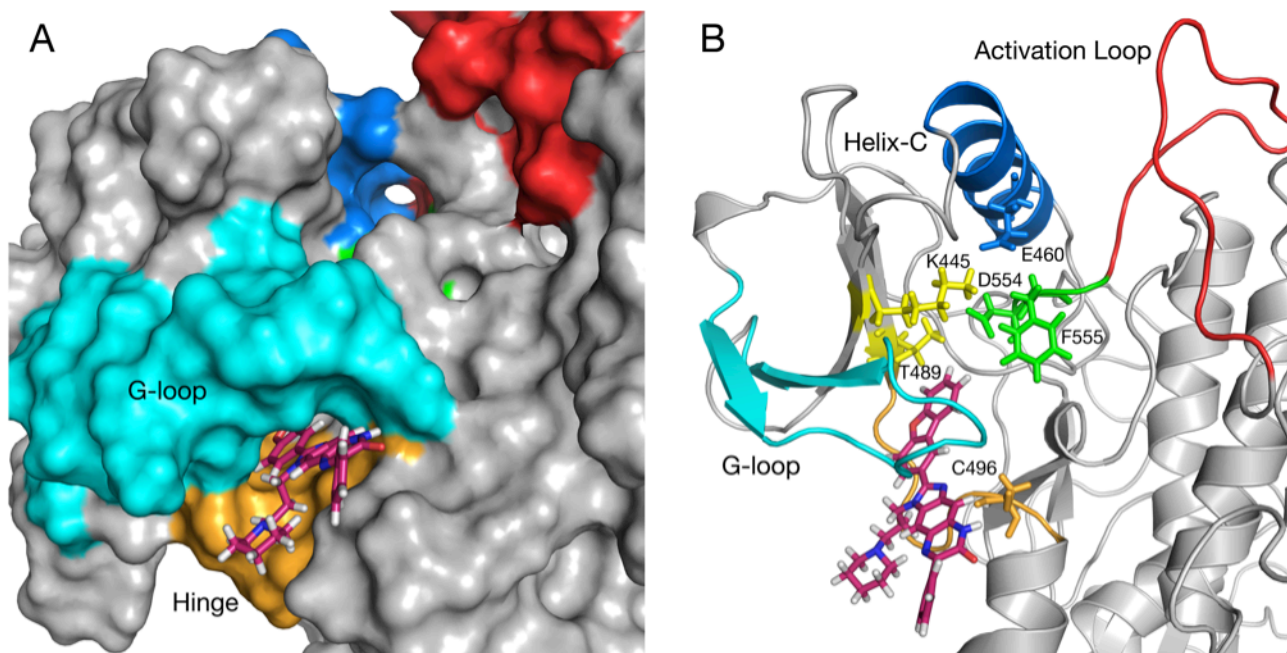


Figure 3: Molecular Modeling of CTA095-Etk docking. (A) Surface view of Etk docked to CTA095 after 20 ns of MD minimization and relaxation. R3 and the three-ring core docked deeper between Glycine-rich loop region (cyan) and hinge region (orange), R1 and R2 are solvent exposed. Blue: Helix C; Red: Activation Loop; Green: DFG motif (554–556); Cyan: Glycine-rich loop; Orange: Hinge Region. (B) Cartoon representation showing predicted interactions of CTA095 with the gatekeeper Thr489, DFG (554–556) motif, and Cys496. CTA095 binding stabilizes Phe555 in 'out' configuration, and affects the active state salt bridge formation between Lys445 and Glu460. Blue: Helix C; Red: Activation Loop; Green: DFG motif (554–556); Cyan: Glycine-rich loop; Orange: Hinge Region. Figures were generated using PyMol.

Our computational pipeline for designing stapled peptides first assembles the peptide backbone using a Monte Carlo Rosetta Fragment assembly method¹², which is followed by placement of covalent crosslinks to constrain the backbone, and sequence design to stabilize the conformation. Thousands of designs are thus generated spanning very diverse shapes and sizes, and are filtered for stability, and their preference for unique folded state. Our preliminary results show that the computational methods are able to design peptides that fold exactly as designed. Thermal stability and chemical denaturation experiments also show that these peptides are extremely stable, and do not melt even when heated to 95 C. We are continuing to improve on these methods, and are now compiling a library of hyperstable scaffolds that can be used to redesign and target Tek kinases such as Etk and Btk.

Taken together, we have used our computational methods to generate and screen virtual small molecule libraries, and identify promising new lead compounds targeting the activity of Tek kinases (specifically Etk). We continue to pursue these methods for generating more diversity and identify better scaffolds and compounds, however we are optimistic that these *in silico* identified compounds will show good inhibitory activity in experimental assays, and thus could serve as lead candidates for new therapeutics against late stage prostate cancer.

Specific Aim 2: Identifying Novel Target Sites for Etk

As part of this aim, we sought to infer phylogenetic for the Tek protein family, and explore novel sites for targeting specific members.

Task 2a: Phylogenetic Inference of the Tek protein family

We used PHYRN¹³ to construct a high-resolution phylogenetic history of the Tek protein family. PHYRN is phylogenetic profile-based approach previously developed by me, and provides better resolution than conventional phylogenetic reconstruction methods. Conserved domains from the Tek protein family are used to generate Position Specific Substitution Matrices (PSSM) library that represents the diversity in sequence space. Pairwise comparisons between the full-length sequences and PSSM library are then used to calculate evolutionary distance matrix, followed by inference of phylogenetic tree based on the calculated distance matrix.

Due to extreme divergence in the domain architecture of Tek family members, initial attempts at generating Phylogenetic trees using PSSMs derived from all the domains did not exhibit good resolution. Therefore, robust and statistically significant phylogenetic trees were constructed using PSSMs derived from the kinase domain. PHYRN-derived phylogenetic trees showed monophyletic relationships for Etk, Itk, Tec and Txk groups (Figure 6). However, most importantly, the phylogenetic studies highlighted the highly conserved nature of kinase domain in Tek protein family. This complicates the matter for design and development of subtype-specific inhibitors. The data from phylogenetic trees can be further analysed to identify distinctive sequence motifs for developing specific inhibitors.

Table1: Energy Profiles of top-scoring hits from CTG-Etk virtual screening

Name	Rosetta Interface Energy (REU)	Autodock Binding Energy
CTA095	-19.288	-7.60
CTG01	-19.287	-10.20
CTG02	-21.473	-11.25
CTG03	-16.877	-10.05
CTG04	-18.369	-9.19
CTG05	-18.582	-8.47
CTG06	-22.017	-10.85
CTG07	-18.784	-9.86
CTG08	16.297	-9.86

Table2: Energy Profiles of top-scoring hits from CTX-Etk virtual screening

Name	Autodock Binding Energy	Cluster Size (Max: 256)
CTX21	-12.89	194
CTX4	-12.25	223
CTX27	-11.96	209
CTX3	-11.89	231
CTX9	-12.08	159
CTX29	-11.5	250
CTX20	-11.07	255
CTX18	-10.49	246
CTX8	-10.03	219

Task 2b: Protein Structural Modeling

Since the ligand bound conformations of Etk, Btk, Itk and other members of Tek protein family are already available in protein data bank, we did not require to model the protein structures. However, since most structures in PDB were in ligand-bound conformation, we minimized the structures using Rosetta scoring function after removing the ligand. Ligand free structures were

also minimized using short (~5ns) MD trajectories. These minimized structures were then used for computational docking and dynamics studies.

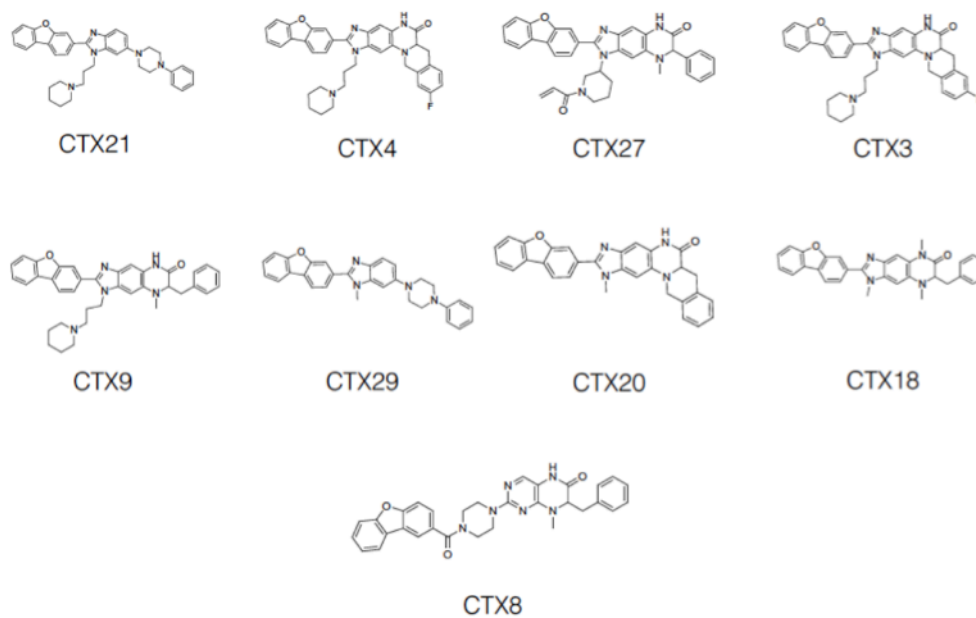


Figure 4: Top-Scoring hits from virtual screening of CTX library

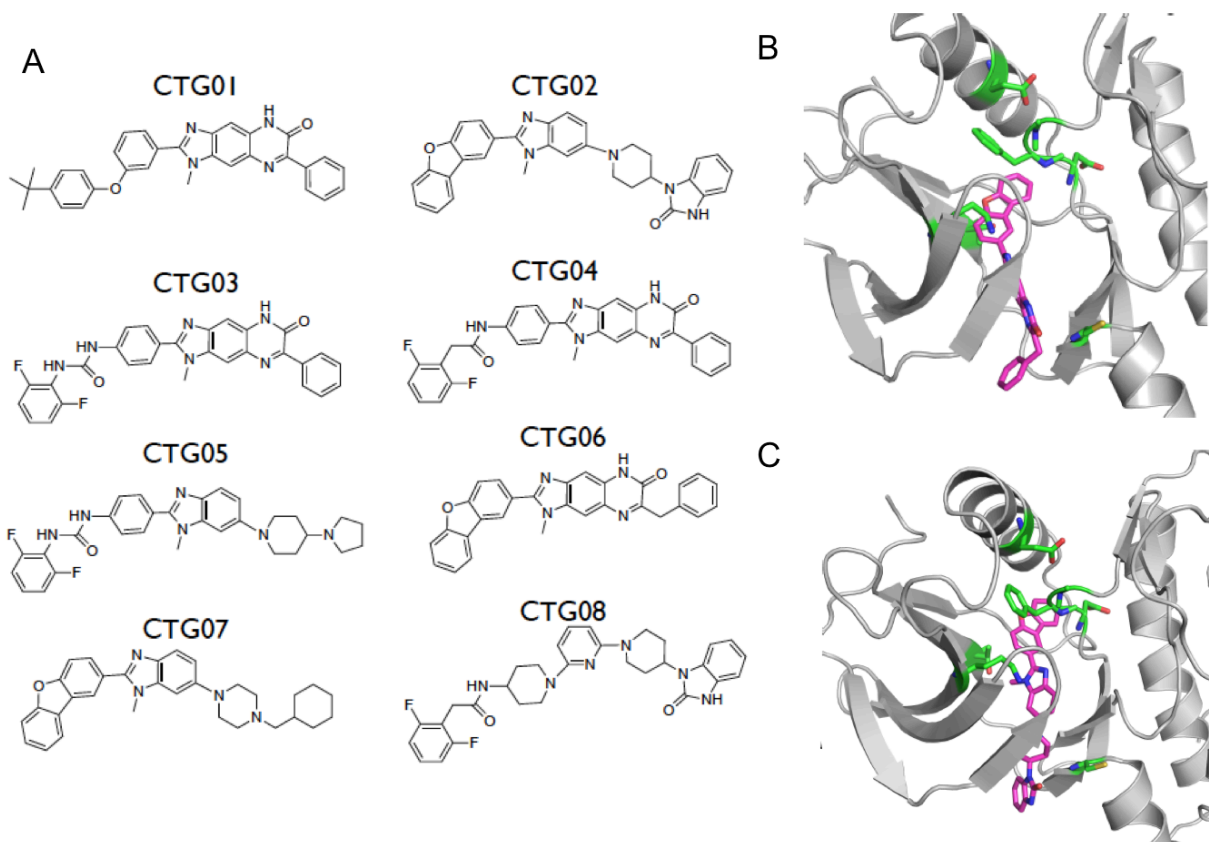


Figure 5: Virtual Screening for Etk binding with CTG library: (A) Chemical Structures of Top Scoring Ligands (B) CTG06 bound to Etk (C) CTG02 bound to ETK

Task 2c: Comparative Sequence and Structure Studies

Sequence and structural alignments between Btk and Etk show that kinase domain is highly conserved, and there are very small changes in the tertiary structure, further highlighting difficulties in designing subtype-selective inhibitors.

Studies on the domain organization of the member show that unique aspect of Tek family is the presence of Pleckstrin Homology (PH) domain (**figure 7**). This domain plays crucial role in the activation and functioning of these kinases. Therefore, it presents attractive opportunities for targeting using peptide-based therapeutics. As described in previous tasks, we are currently pursuing this using hyperstable constrained peptides rationally designed using novel Rosetta peptide-design methods.

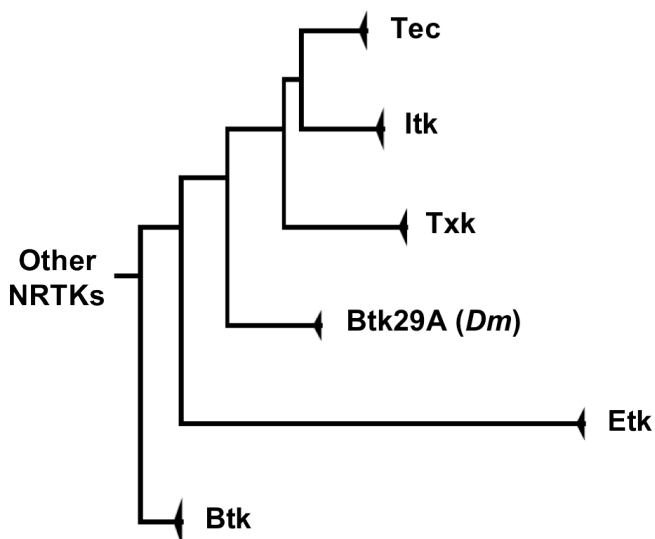


Figure 6: Representative Phylogenetic Tree of Tec Family inferred using PHYRN. Resampling support for deep nodes > 80%

Specific Aim 3: Experimental Validation of *in-silico* predictions.

Computationally designed and *in silico* screened ligands were experimentally synthesized and tested for their effect on growth and proliferation of prostate cancer cells. Our experiments show that these variants of CTN06 and CTA095 show promising inhibitory activity on the growth and proliferation of prostate cancer cell lines.

Task 3a: Synthesis of novel small molecule inhibitors

Multiple variants of CTN06 and CTA095 that passed *in silico* filters were synthesized as previously described by our group^{7,8}. We continue to iterate between *in silico* screening and synthesis and testing of new designs.

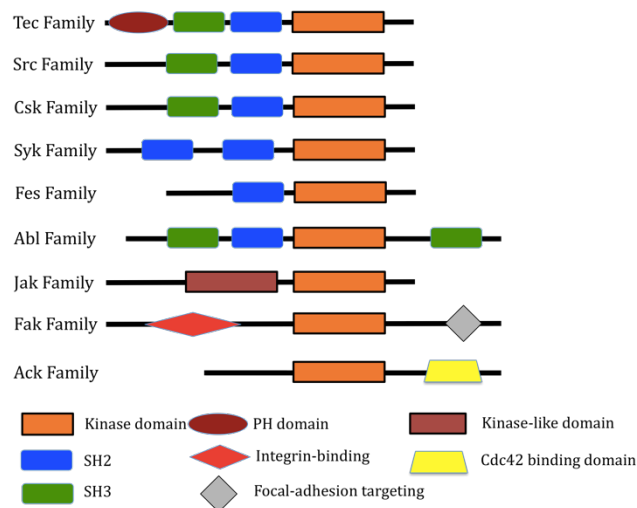


Figure 7: Domain Architecture of the Tek Family Members

Task 3b: Effect on Cell Growth and Proliferation

Growth inhibition studies were performed with CTN06 and CTA095 variants that passed *in silico* filters and were synthesized successfully. PC3 cells were used for MTT assay to evaluate the effect of our novel small molecule compounds on growth of PC3 cells. Our preliminary studies show that some of the CTN and

CTA variants, specifically, CTN18, CTA201, CTA202 and CTA205 show growth inhibition comparable to CTA095 (Figure 8).

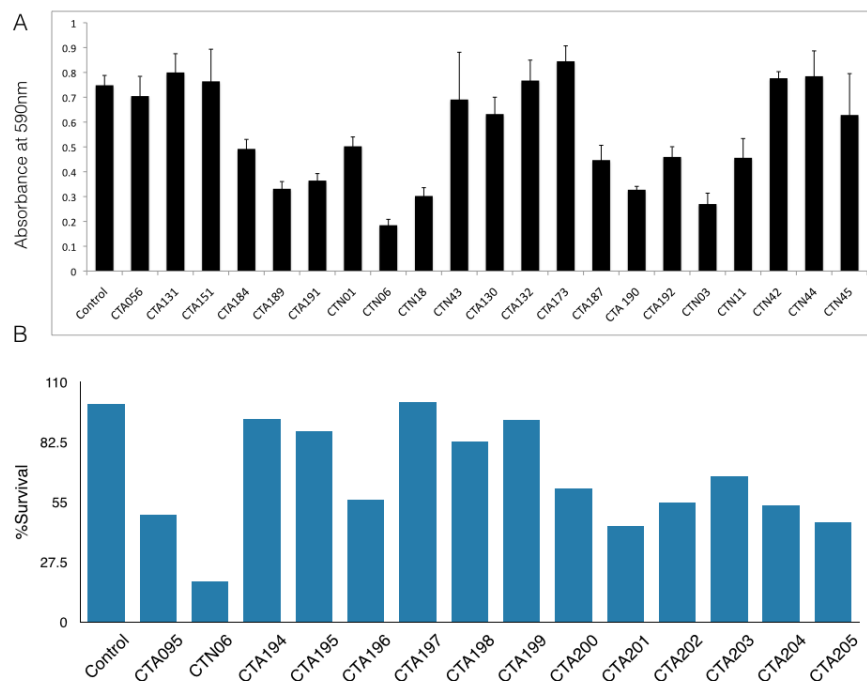


Figure 8: Effect of designed compounds on Cell survival in PC3 cells. A) X axis shows the absorbance at 590 nm measured at the end of MTT assay B) cell survival normalized according control treatments.

Taken together, our preliminary results are indicative that the novel compounds identified from *in silico* screens negatively affect the growth and proliferation of prostate cancer cell lines. Future studies will focus on the further biochemical characterization of these inhibitors. Also, a major focus of our work will be to develop peptide-based therapeutics for developing subtype-specific inhibitors.

KEY RESEARCH ACCOMPLISHMENTS

- Computational docking and dynamics revealed the binding mode and mechanism of action for CTN06 and CTA095 compounds that target members of the Tek kinase family.
- Virtual libraries of CTN06 and CTA095 variants were generated, and screened using *in silico* methods to identify multiple novel inhibitors of Etk.
- Phylogenetic and structural comparison studies have identified unique signatures and domains for the members of Tek kinase family.
- Computational methods for design of constrained peptides have been developed.
- Hyperstable constrained peptide scaffolds have been constructed and characterized for redesign to bind Etk-specific PH domain.

- Experimental studies with small molecule ligands identified from the computational screens show promising growth inhibition effects in experimental studies.

Conclusion

We have developed computational frameworks to support combinatorial searches of small molecule inhibitors that target the members of Tek kinase family. Specifically, we used computational molecular docking to decipher the mechanism of action for CTN06 and CTA095, which inhibit kinase activity of Btk and Etk kinase. Both these kinase play key roles in the growth and proliferation of prostate cancer cells; therefore both these inhibitors present significant opportunities to control prostate cancer growth *in vivo*. We sought to develop better inhibitors of these Tek kinase using computational and combinatorial frameworks. The information derived from the docking studies of CTN06/CTA095 was used to design virtual libraries of their variants. Following large scale computational screens employing computational docking and molecular dynamics, multiple new small molecule ligands with potential inhibitory activity were identified. Indeed, the experimental data on these variants suggests some of these variants do show significant inhibition of PC3 cell growth. We continue to validate and characterize these variants, and will focus on further improving these ligands in future.

Another major focus of our work now is to focus on developing subtype specific inhibitors. However, as our phylogenetic and structural studies showed, there are very high similarities between Btk, Etk and other kinases such as Itk, Src etc. This makes it a very challenging to target the kinase domain specifically with small molecule ligands. Therefore, we are pursuing design of constrained peptide-based inhibitors against these kinases. We are currently working on method development for design of constrained peptides with precise control over their shape and size. The methods developed and stable peptide scaffolds developed through this methods are being used for rational design of these therapeutics to target unique structural motifs of these kinases. More generally, we have shown that computational methods can be significantly complement conventional experimental-based search of novel therapeutics.

PUBLICATIONS, ABSTRACTS AND PRESENTATIONS

- **“Targeting Btk/Etk of prostate cancer cells by a novel dual inhibitor”** by W Guo, R. Liu, **G Bhardwaj**, JC Yang, C changou, A-H Ma, A Mazloom, S Chintalpalli, K Xiao, W Xiao, P Kumaresan, E Sanchez, C-T Yeh, CP Evans, R Patterson, KS Lam, H-J Kung, ***Cell Death and Disease*** (2014) 5, e1409
- **“Building a Haystack, and Finding the Needle: Combinatorial and Computational Approaches for Developing Anti-Cancer Therapeutics”** Presentation by **Gaurav Bhardwaj** at Institute of Protein Design, University of Washington, Seattle. (March 2014)
- **“Computational Design of Tec Kinase Inhibitors”**-Presentation by **Gaurav Bhardwaj** at the UC Davis Stand Up To Cancer (SU2C) Dream Team Meeting (October 2013)
- **“Accurate Computational Design of heterochiral constrained peptides”** Presentation by Gaurav Bhardwaj at Cyrus Biotechnology, Seattle (April 2016).

- **“De novo design of cyclic peptides”**-Poster presentation by Gaurav Bhardwaj at RosettaCon 2015

INVENTIONS, PATENTS AND LICENSES

Nothing to Report

REPORTABLE OUTCOMES

- A paper (co-authored by me) outlining the role of CTN06 in dual inhibition of Btk and Etk, was published in journal Cell Death and Disease
- Multiple new Etk inhibitors were identified through computational design and screening and are being developed further.
- Methods for computational design hyperstable constrained peptides are being developed.

TRAINING PROGRAM

As proposed in the original submission, I continue to focus on the training aspects targeted towards developing my experimental skills to complement my computational training. During the last funding period, I have learned and worked significantly on solid phase methods for peptides and small molecule production. Besides the synthesis aspects, I have also focused on biochemical characterization of stability and structure of these novel molecules, and biological assays to study their effects on growth and proliferation of cell-based assays.

Since the last active funding period, I have moved to David Baker's group at University of Washington, Seattle. Dr. Baker's group is world leader in computational protein design, and my training has hugely benefitted from the transfer. I have acquired new skill set on computational protein design using Rosetta software suite, which I have successfully applied to designing small, hyperstable constrained peptides. The ultimate goal for these designed peptides is to use them as scaffolds for designing selective binders of Tek kinases.

I have continued to regularly discuss my progress with my mentors, and have forged multiple new collaborations. I have also had the opportunity to present my work at multiple national and international conferences, including RosettaCon in 2014 and 2015. These meetings helped me get broader feedback on my project as well as suggestions on how to improve on my computational and experimental pipeline.

Overall, work related to this project has contributed significantly to my training, as I make progress towards an independent position in future.

REFERENCES

1. Dai, B. *et al.* Tyrosine kinase Etk/BMX is up-regulated in human prostate cancer and its overexpression induces prostate intraepithelial neoplasia in mouse. *Cancer Res.* **66**, 8058–8064 (2006).
2. Xue, L. Y., Qiu, Y., He, J., Kung, H. J. & Oleinick, N. L. Etk/Bmx, a PH-domain containing tyrosine kinase, protects prostate cancer cells from apoptosis induced by photodynamic therapy or thapsigargin. *Oncogene* **18**, 3391–3398 (1999).
3. Wen, X., Lin, H. H., Shih, H. M., Kung, H. J. & Ann, D. K. Kinase activation of the non-receptor tyrosine kinase Etk/BMX alone is sufficient to transactivate STAT-mediated gene expression in salivary and lung epithelial cells. *J. Biol. Chem.* **274**, 38204–38210 (1999).
4. Tsai, Y. T. *et al.* Etk, a Btk family tyrosine kinase, mediates cellular transformation by linking Src to STAT3 activation. *Mol. Cell. Biol.* **20**, 2043–2054 (2000).
5. Wu, Y. M., Huang, C. L., Kung, H. J. & Huang, C. Y. Proteolytic activation of ETK/Bmx tyrosine kinase by caspases. *J. Biol. Chem.* **276**, 17672–17678 (2001).
6. Chen, K.-Y., Huang, L.-M., Kung, H.-J., Ann, D. K. & Shih, H.-M. The role of tyrosine kinase Etk/Bmx in EGF-induced apoptosis of MDA-MB-468 breast cancer cells. *Oncogene* **23**, 1854–1862 (2004).
7. Guo, W. *et al.* Targeting Btk/Etk of prostate cancer cells by a novel dual inhibitor. *Cell Death Dis.* **5**, e1409 (2014).
8. Guo, W. *et al.* CTA095, a novel Etk and Src dual inhibitor, induces apoptosis in prostate cancer cells and overcomes resistance to Src inhibitors. *PLoS One* **8**, e70910 (2013).
9. Morris, G. M. *et al.* AutoDock4 and AutoDockTools4: Automated docking with selective receptor flexibility. *J. Comput. Chem.* **30**, 2785–2791 (2009).
10. Combs, S. A. *et al.* Small-molecule ligand docking into comparative models with Rosetta. *Nat. Protoc.* **8**, 1277–1298 (2013).

11. Phillips, J. C. *et al.* Scalable molecular dynamics with NAMD. *J. Comput. Chem.* **26**, 1781–1802 (2005).
12. Huang, P.-S. *et al.* RosettaRemodel: a generalized framework for flexible backbone protein design. *PLoS One* **6**, e24109 (2011).
13. Bhardwaj, G. *et al.* PHYRN: a robust method for phylogenetic analysis of highly divergent sequences. *PLoS One* **7**, e34261 (2012).

Targeting Btk/Etk of prostate cancer cells by a novel dual inhibitor

W Guo¹, R Liu^{*1}, G Bhardwaj¹, JC Yang², C Changou¹, A-H Ma¹, A Mazloom¹, S Chintapalli^{1,3}, K Xiao¹, W Xiao¹, P Kumaresan¹, E Sanchez¹, C-T Yeh⁴, CP Evans², R Patterson^{1,3}, KS Lam¹ and H-J Kung^{*,1,5}

Btk and Etk/BMX are Tec-family non-receptor tyrosine kinases. Btk has previously been reported to be expressed primarily in B cells and has an important role in immune responses and B-cell malignancies. Etk has been shown previously to provide a strong survival and metastasis signal in human prostate cancer cells, and to confer androgen independence and drug resistance. While the role of Etk in prostate carcinogenesis is well established, the functions of Btk in prostate cancer have never been investigated, likely due to the perception that Btk is a hematopoietic, but not epithelial, kinase. Herein, we found that Btk is overexpressed in prostate cancer tissues and prostate cancer cells. The level of Btk in prostate cancer tissues correlates with cancer grades. Knockdown of Btk expression selectively inhibits the growth of prostate cancer cells, but not that of the normal prostate epithelial cells, which express very little Btk. Dual inhibition of Btk and Etk has an additive inhibitory effect on prostate cancer cell growth. To explore Btk and Etk as targets for prostate cancer, we developed a small molecule dual inhibitor of Btk and Etk, CTN06. Treatment of PC3 and other prostate cancer cells, but not immortalized prostate epithelial cells with CTN06 resulted in effective cell killing, accompanied by the attenuation of Btk/Etk signals. The killing effect of CTN06 is more potent than that of commonly used inhibitors against Src, Raf/VEGFR and EGFR. CTN06 induces apoptosis as well as autophagy in human prostate cancer cells, and is a chemo-sensitizer for docetaxel (DTX), a standard of care for metastatic prostate cancer patients. CTN06 also impeded the migration of human prostate cancer cells based on a 'wound healing' assay. The anti-cancer effect of CTN06 was further validated *in vivo* in a PC3 xenograft mouse model.

Cell Death and Disease (2014) 5, e1409; doi:10.1038/cddis.2014.343; published online 4 September 2014

Prostate cancer is the most frequently diagnosed cancer and the second leading cause of cancer deaths in men in the United States.¹ The risk and side effects associated with current therapies, which range from impotence and incontinence after surgery to recurrence of an androgen-independent tumor after androgen ablation therapy, are severe. Tyrosine kinase inhibitors (TKIs) are among the most promising targeted therapies, most of which are directed against receptor tyrosine kinases. The outcomes of clinical trials based on TKIs as single agents have generally been modest, probably due to redundancy in receptor binding and signaling to intracellular mediators.²

The Tec family of tyrosine kinases is the second largest family of cytoplasmic tyrosine kinases. It consists of six members with tissue-specific expression patterns in normal cells. Btk is the prototype of this family of tyrosine kinases. Btk is reportedly expressed primarily in B cells, monocytes, macrophages and neutrophils,³ as well as in B-cell malignancies. In addition to being a critical effector for the B-cell

receptor,⁴ Btk engages B-cell Toll-like receptors (e.g., TLR2 and TLR4)^{5,6} and FAS.³ Btk is activated by SFK (src family kinases) and Syk, and transmits signals to PI3K and PLC-gamma, resulting in a calcium flux and the activation of NF-κB and NFATc transcriptional factors.^{7,8} The role of Btk in the immune response and hematopoietic malignancies has been well studied. Deficiency of Btk in humans leads to X-linked agammaglobulinemia (XLA).⁴ Btk has been reported as an anti-apoptotic protein in neutrophils and macrophages. Btk-deficient neutrophils have increased production of ROS and stimulation-induced apoptosis.³ Knockdown of Btk in macrophages led to increased LPS and TNF-induced apoptosis.⁶ Btk also has an important role in arthritis, leukemia and lymphoma. Several Btk inhibitors have been reported including LFM-A13, a reversible Btk inhibitor through rational design,⁹ and PCI32765, an irreversible Btk inhibitor. PCI-32765 has shown encouraging effect in clinical studies for treatment of chronic lymphocytic leukemia and in collagen-induced arthritis mouse model.^{10–12} These inhibitors also

¹Department of Biochemistry and Molecular Medicine, University of California Davis, Sacramento, CA 95817, USA; ²Department of Urology, University of California Davis, Sacramento, CA 95817, USA; ³Department of Physiology and Membrane Biology, University of California Davis, Sacramento, CA 95817, USA; ⁴Department of Medical Research and Education, Taipei Medical University-Shuang Ho Hospital, Taipei, Taiwan, ROC and ⁵Institute of Molecular and Genomic Medicine, National Health Research Institutes (NHRI), Miaoli County 35053, Taiwan, ROC.

*Corresponding authors: R Liu, Department of Biochemistry and Molecular Medicine, University of California Davis, 2700 Stockton Boulevard, Suite 2301, Sacramento, CA 95817, USA. Tel: +916 734 6414; Fax: +916 734 6415; E-mail: rliu@ucdavis.edu

or H-J Kung, Department of Biochemistry and Molecular Medicine, UC Davis Cancer Center, 4645 2nd Avenue, Research III, Rm 2400D, Sacramento, CA 95817, USA. Tel: +916 734 1538; Fax: +916 734 2589; E-mail: hkung@ucdavis.edu or Institute of Molecular and Genomic Medicine, National Health Research Institutes (NHRI), No. 35, Keyan Road, Zhunan Town, Miaoli County 35053, Taiwan, ROC. Tel: +886 37 246 166 ext. 31000; Fax: +886 37 586 402; E-mail: hkung@nhri.org.tw

Abbreviations: CTN06, N-(7-isobutyl-6-oxo-1-(3-(piperidin-1-yl)propyl)-5,6-dihydro-1H-imidazo[4,5-g]quinoxalin-2-yl)-4-(pyridin-4-yl)benzamide; Btk, Bruton's tyrosine kinase; Etk, Endothelial and epithelial tyrosine kinase; XLA, X-linked agammaglobulinemia; TKIs, tyrosine kinase inhibitors; CLL, chronic lymphocytic leukemia; SFK, Src family kinases; CQ, chloroquine; DTX, docetaxel; pBTK, phospho-Btk

Received 08.4.13; revised 22.6.14; accepted 13.7.14; Edited by G Ciliberto

exhibited potential in targeting multiple myeloma in the bone marrow microenvironment.¹³ Although these inhibitors greatly broadened the scope for potential Btk targeting in human diseases, reactivity of irreversible inhibitor with other proteins remains a concern. As a result, the development of a potent, reversible Btk inhibitor is highly desirable.

As described above, most reported studies of Btk focused on the hematopoietic system; however, the role of Btk in solid tumors remains unknown. By contrast, Etk (also called BMX), another member of Tec family, has been shown to be expressed in epithelial and endothelial cells, and is involved in the development or treatment resistance of several epithelial malignancies.^{14–16} It is overexpressed in human prostate cancer specimens, and provides strong survival functions in prostate cancer cells.^{17,18} Overexpression of Etk induces prostate intraepithelial neoplasia in mice,¹⁹ and knockout of Etk in an endothelial lineage decreases tumor angiogenesis and growth.²⁰ We showed previously that Etk forms a complex with Src and FAK, and that it is an effective activator of STAT3.^{21,22} In prostate cancer cells, it is activated by EGFR and erbB3,²³ as well as IL-6 and neuropeptides, leading to aberrant activation of androgen receptor.²⁴ Etk sequesters p53 and confers survival and therapeutic resistance.²⁵ In glioblastoma, Etk was found to be critical in maintaining the

self-renewal and tumorigenic potential of cancer stem cells through Stat3 activation.²⁶ Therefore, systemic inhibition of Etk may offer a synergistic anti-tumor effect. As of yet, there is no efficacious inhibitor for this kinase.

Herein, we report that Btk is also aberrantly expressed in prostate cancer. Moreover, a novel Btk and Etk dual inhibitor, CTN06, was identified. CTN06 induces autophagy and apoptosis in prostate cancer cells, and inhibits prostate cancer xenograft tumor growth *in vivo*. To our knowledge, this is the first report of the role of Btk in solid tumors, and also the first report of a novel Btk/Etk dual inhibitor with an application as an anti-cancer agent.

Results

Btk is expressed at high levels in prostate cancer. Etk has previously been reported to be overexpressed in prostate cancer, and it promotes growth, survival and angiogenesis of prostate cancer.^{19,27} Btk, the closest member of Etk in the human kinome, was mainly reported in hematopoietic cells and B-cell malignancies. The role of Btk in solid cancers remains unknown. Using a tissue microarray assay, we found that Btk is overexpressed in prostate cancer tissues. Significantly, the expression level

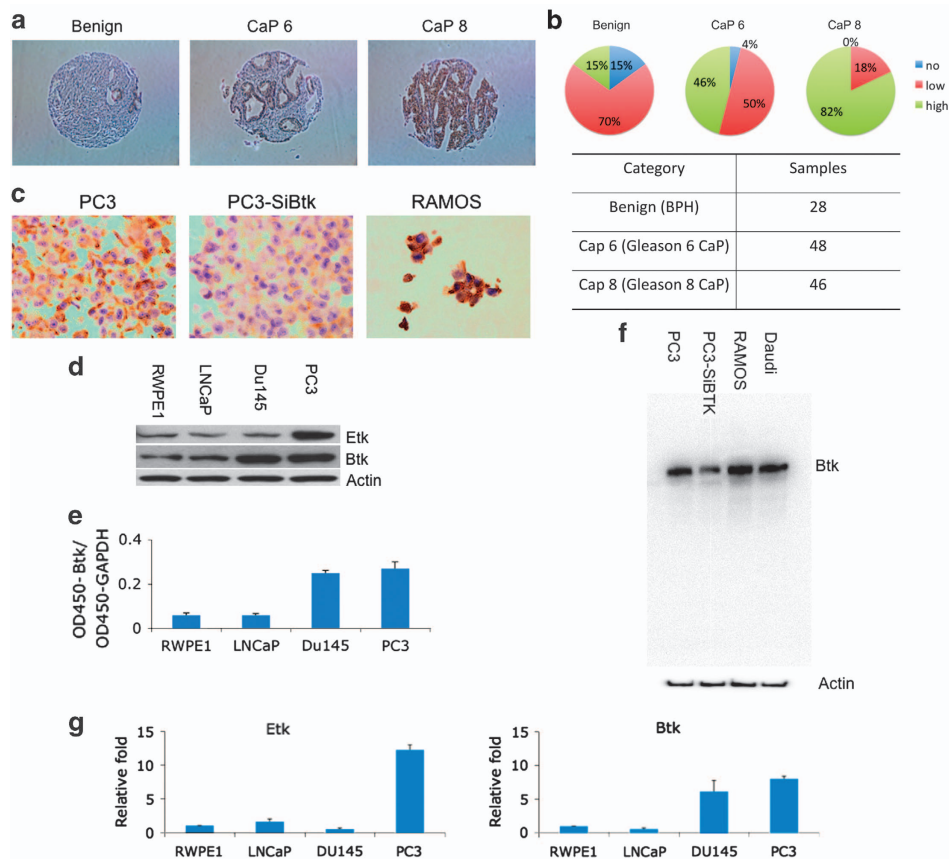


Figure 1 BTK is expressed in prostate cancers and cell lines. (a) The expression level of Btk in prostate cancer tissue was examined using tissue microarray. (b) The array contains 28 benign, 48 gleason 6 (CaP 6) and 46 gleason 8 (CaP 8) prostate cancer samples. (c) The antibody used was confirmed using cellblocks with PC3, PC3 with depletion of Btk by SiBtk and RAMOS cells. (d) The expression level of Etk and Btk in prostate cancer cells was examined using western blot assay. (e) Btk levels in prostate cancer cells were also measured using ELISA. (f) The antibody for tissue microarray was also confirmed using western blot with RAMOS cells and siBtk for PC3 cells, and with Daudi cells as a positive control. (g) Btk levels were further confirmed using RT-PCR. Columns, mean; bars, standard deviation, $n = 3$

of Btk correlates with the grade of prostate cancer (Figures 1a and b). The antibody used for tissue microarray was confirmed using cell blocks with RAMOS cells as a positive control (Figure 1c). In addition to the tissue microarray, the expression level of Etk and Btk in prostate cancer cells LNCaP, Du145, PC3 and immortalized normal prostate cell RWPE1 was examined using western blots. Etk was found to be high in PC3 cells, and Btk was found to be high in both Du145 and PC3 cells, a similar expression pattern compared with the tissue microarray (Figure 1d). Btk levels in RWPE1, LNCaP, Du145 and PC3 cells were further measured using ELISA (Figure 1e). The specificity of the Btk antibody used was validated by the decreased Btk level, when Btk was knocked down by siRNA targeting Btk in PC3 cells, as well as in RAMOS cells which served as a positive control (Figure 1f). The elevated mRNA levels of Etk and Btk in those cells were also observed, using real-time RT-PCR, which indicates the overexpression of Etk and Btk in prostate cancer cells is at least in part at the transcriptional level (Figure 1g).

Simultaneous knockdown of Etk and Btk inhibits prostate cancer cell growth. Etk knockdown has been reported to slow down prostate cancer cell growth. A similar result was observed in PC3 cells with Etk knockdown (Figure 2a). To explore the role of Btk in prostate cancer cell growth, the Btk level in PC3 prostate cancer cells was knocked down using siRNA. Btk knockdown in PC3 cells showed a similar inhibitory effect on prostate cancer cell growth as compared with Etk knockdown. Simultaneous knockdown of Etk and Btk resulted in a much greater inhibitory effect on prostate cancer cell growth when

compared with Etk or Btk knockdown alone (Figure 2a). In stark contrast, RWPE1, the immortalized normal prostate cell line, is resistant to Etk and Btk knockdown (Figure 2b), indicating an Etk/Btk 'addiction' of the prostate cancer cells. The effect of Btk to prostate cancer cell growth was further examined in PC3 cells and Du145 cells using SiBtk and LFM-A13, a known Btk inhibitor. Both approaches inhibited prostate cancer cell growth at a similar level, further confirming an important role of Btk in prostate cancer cell growth (Figure 2c).

CTN06 as a dual inhibitor against Btk and Etk tyrosine kinases. Having identified a tumor-specific role of Btk and Etk in prostate cancer, we attempted to develop inhibitors targeting this family of kinases. Through screening a 9600-diversity combinatorial solution phase small molecule library, hit compounds with inhibitory activities against Etk were discovered. Subsequent optimization led to the identification of CTN06 (Figure 3a). To determine the substrate specificity of this compound, purified Etk, Btk, Src and Mer were incubated in a kinase reaction buffer with CTN06 (0–10 μ M) in the presence of 33 P-labeled ATP and a peptide (YIYGSFK), previously shown to be an excellent substrate for both Btk and Src family kinases. The kinase activity was measured using the thin-layer chromatography (TLC) technique. CTN06 was found to be an even more potent Btk inhibitor with an IC_{50} of ~ 50 nM compared with Etk ($IC_{50} \sim 200$ nM) (Figure 3b). Inhibition was observed in a concentration-dependent manner. Src ($IC_{50} \sim 5$ μ M) and Mer ($IC_{50} > 10$ μ M) were significantly more resistant to CTN06 inhibition (Figures 3b and c).

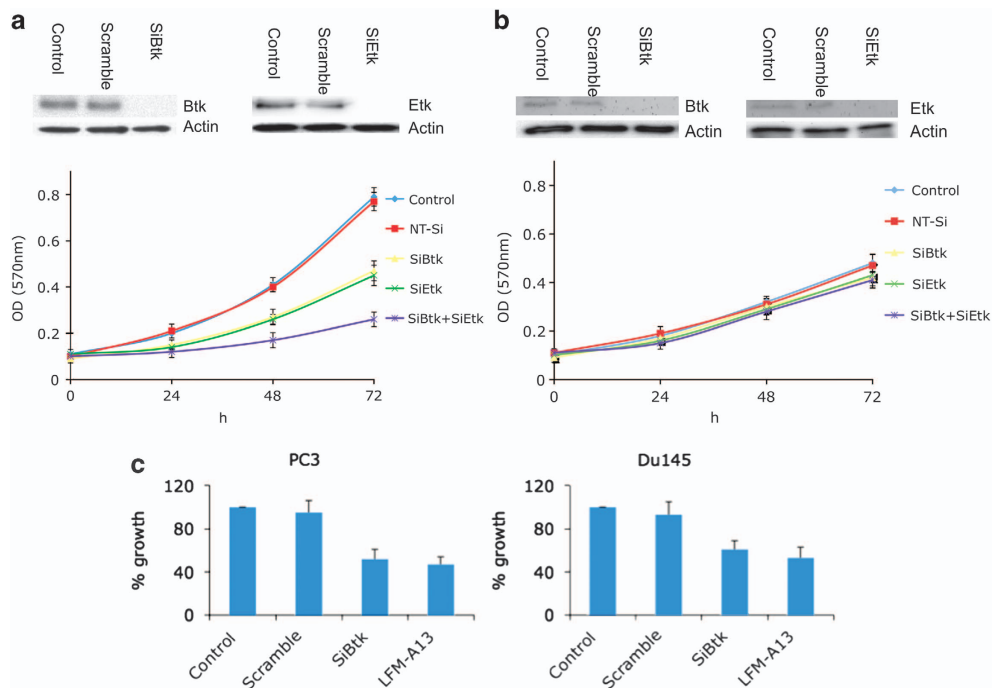


Figure 2 Both Btk/Etk (BMX) contribute to proliferation of prostate cancer cells. (a and b) The expression of Etk and Btk in PC3 and RWPE1 cells was knocked down using the corresponding siRNA. The growth of the knockdown cells was measured using MTT assay. (c) The effect of Btk on prostate cancer cell growth was further confirmed using siBtk and LFM-A13 (50 μ M) in PC3 and Du145 cells. Columns, mean; bars, standard deviation, $n = 3$

In addition to the Btk family tyrosine kinases, the inhibitory activity of CTN06 against other tyrosine kinases, including Itk, Lyn, Axl, Mer, EGFR and Abl, was investigated using the TLC assay. CTN06 appears to have the strongest activity toward Btk and Etk, followed by Itk, another member in the same family. No significant inhibitory activity toward any other kinases was observed (Figure 3d).

The inhibitor specificity is supported by the molecular docking studies. CTN06 is found to bind to the pocket of the ATP binding site with a binding energy of -11 kcal/mol (Figures 3e and f). Previous studies have shown kinase inhibitors that bind to this pocket.^{28,29} Further analysis through molecular dynamics reveals that CTN06 interacts with the 'gatekeeper' residue T474. CTN06 also interacts with the side

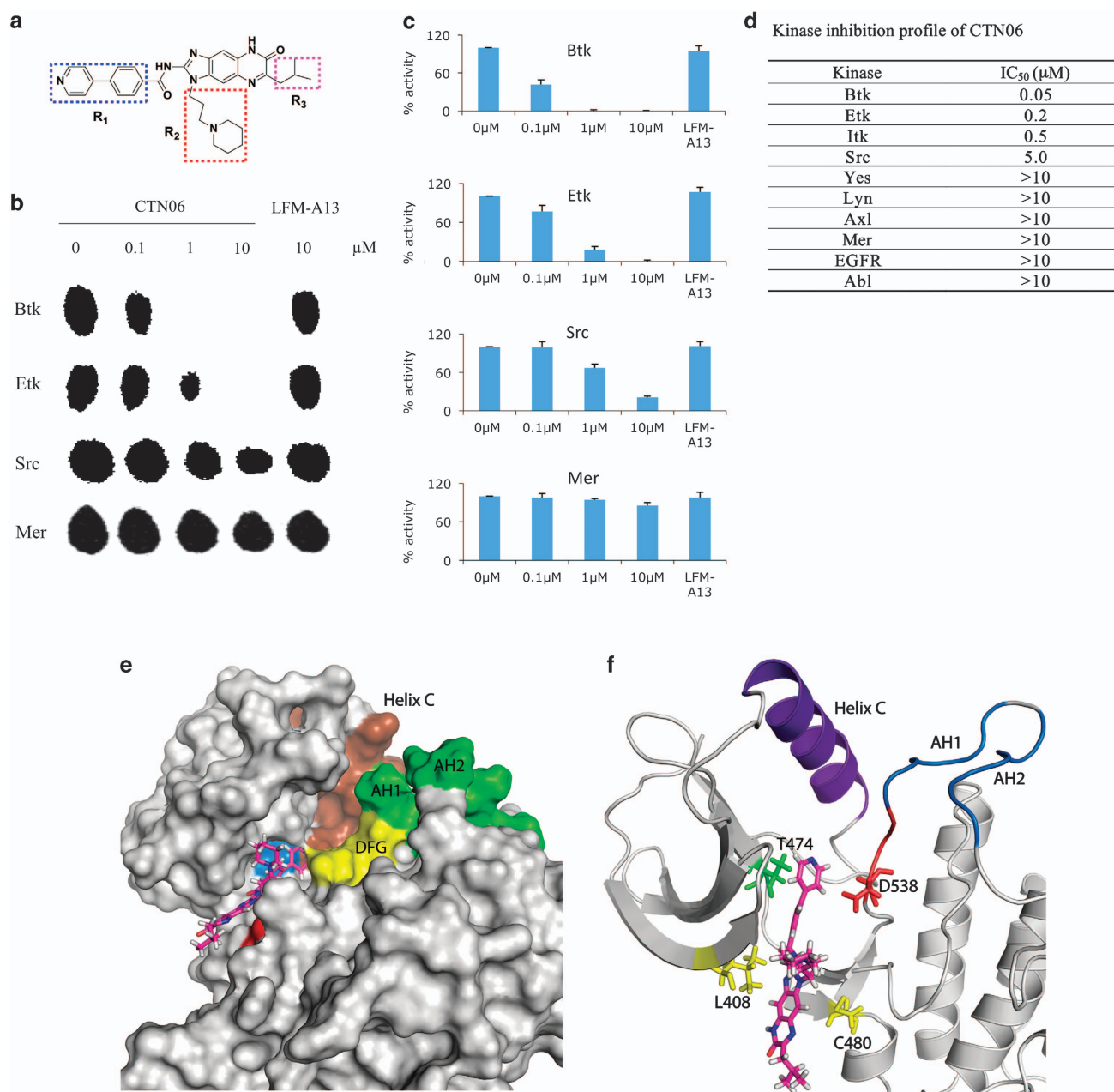


Figure 3 CTN06 is a potent Etk and Btk dual inhibitor. **(a)** Chemical structure of CTN06. **(b)** The potency of CTN06 to Btk, Etk, Src and Mer was measured using TLC to identify 32 P-phosphorylated peptide substrate. Purified TKs (20 nM), CTN06 (0–10 μ M) and the peptide substrate (YIYGSFK) were incubated with 32 P-ATP in a kinase reaction. The resulting product was analyzed on a TLC plate. **(c)** The intensity of the radioactive spot was measured using densitometer. **(d)** Summarization of the kinase inhibition profile of CTN06. Columns, mean; bars, standard deviation, $n=3$. Molecular docking of CTN06 to Btk. **(e)** Surface view of Btk docked to CTN06 after 20 ns of MD relaxation. Brown: helix C (439–452); green: activation loop helix 1 (AH1) (541–546) and activation loop helix 2 (AH2) (548–553); yellow: DFG motif (538–540); blue: Thr474; red: Cys480. **(f)** Cartoon representation showing predicted interactions of Btk with CTN06. Thr474, Leu408, Cys480 and Asp538 side chains are shown as sticks and colored based on residue type (red: acidic, green: polar, yellow: non-polar). DFG motif is shown in red. Figures were generated using PyMol

chains of C480, which is a residue unique to Btk when compared with other kinases. Previous studies have shown that only 8 kinases out of 491 that show T474 and C480 combination at these positions.²⁸ Molecular dynamics studies reveal that CTN06-Btk binding is stable. We analyzed the molecular dynamics trajectories (Supplementary movie) and plotted putative hydrogen bonding and hydrophobic interactions between CTN06-Btk using LigPlot+ (Supplementary Figure S2). CTN06 putatively forms multiple hydrophobic interactions with side chains of the pocket. The R₁ group interacts with T474, as well as the DFG motif that is important for kinase activity. R₂ and the three-ring core interact with the Glycine-rich loop region, as well as C480. Overall, computational studies show that CTN06 binds to Btk in a stable manner, and the interactions with the back pocket, gate-keeper threonine and the DFG motif lead to its kinase inhibitory properties.

CTN06 preferentially inhibits the growth of malignant prostate cells. To determine the effect of CTN06 on proliferation, a panel of cancer cell lines including LNCaP, Du145, PC3 and the immortalized normal prostate epithelial cell line, RWPE1, were incubated with CTN06 and their proliferation was measured using the MTT assay. CTN06 was very effective in inhibiting the growth of prostate cancer cells (PC3, Du145 and LNCaP), while RWPE1 was much more resistant to CTN06. The ability of CTN06 to inhibit Btk activation, based on phospho-Btk (pBTK) expression in those cells was confirmed using western blot (Figure 4a).

CTN06 induces autophagy in prostate cancer cells. Previously, we showed that the Src inhibitor AZD0530 induces autophagy in prostate cancer cells, which contributes to apoptosis resistance and diminishes the efficacy of the Src inhibitor.³⁰ To determine whether CTN06 can trigger autophagy, PC3 cells stably transfected with GFP-LC3 were treated with CTN06 and then examined under fluorescence microscopy. After 2 and 24 h treatment with CTN06, these cells yielded extensive, distinct 'puncta' autophagosome morphology, whereas vehicle treatment did not. The ability of CTN06 to induce autophagy in PC3 cells was further confirmed by the conversion of endogenous LC3-I to the lipidated LC3-II forms. Addition of chloroquine (CQ), an autophagy blocker and lysosomal disruptor, resulted in the accumulation of larger autophagosomes, suggesting CTN06's effect is on the induction of autophagosome formation (Figure 4b).

CTN06 induces apoptosis in prostate cancer cells. To determine whether the growth inhibition induced by CTN06 on prostate cells was due to apoptosis, flow-cytometric analysis was carried out. Following treatment with CTN06 for 24 h, a dose-dependent accumulation of a 'sub-G1' fraction was observed using propidium iodide (PI) staining. Data based on Annexin-V reactivity also indicated a dose-dependent increase in apoptosis of PC3 cells following treatment with CTN06 (Figure 4c). The 'sub-G1' fraction only measures dead cells with DNA content loss, which may explain why it was less than the percentage of apoptotic cells measured by Annexin-V.

CTN06 inhibits prostate cancer cell migration. Tec-family tyrosine kinases have been shown to have an important role in cellular movement and cancer metastasis. To explore the ability of CTN06 to inhibit cell migration, 'wound healing' of PC3 cells was measured following treatment with CTN06. As shown in Supplementary Figure S3, 'wound healing' of PC3 cells was greatly inhibited by CTN06 after 16 h. These results suggest that CTN06 has the ability not only to suppress prostate cancer cell growth, but also to inhibit cell migration, implicating CTN06 as an anti-metastasis agent.

CTN06 inhibits the phosphorylation of Btk, Etk and the downstream signal PLC γ 2, Stat3, Akt in prostate cancer cells. The inhibitory activity of CTN06 against phosphorylation of Etk and Btk in intact cells was examined by western blot. Btk as well as Etk phosphorylation in PC3 cells were significantly inhibited at 0.5 and 2 μ M. The pPLC γ 2 inhibition is likely to result from Btk inhibition. A selective target for Etk is STAT3,³¹ whose phosphorylation is also inhibited by CTN06, so is Akt, another important downstream effector of Etk (Figure 5). Interestingly, Src phosphorylation was greatly inhibited in cells following treatment with CTN06 compared with kinase inhibition assay. This may be due to inhibition of Etk, which has been shown to cross activate Src.²¹

CTN06 modulates cancer-related miRNAs. Many miRNAs have been reported to have a role in carcinogenesis. To explore whether CTN06 modulates miRNAs, 272 miRNA levels in PC3 cells were examined using a microarray assay following treatment with CTN06. Among them, 22 exhibited alterations >2 folds, for most of which, there are no established functions in oncogenesis (Supplementary Figure S4a). A number of them, however, are known to possess oncogenic and tumor suppressive properties. We found that those miRNAs with tumor suppressive properties were generally upregulated, and those with oncogenic properties were downregulated following treatment with CTN06 (Supplementary Figure S4b).^{32–43} For instance, Mir-132, which is upregulated 29.9 folds following treatment with CTN06, has been reported to be downregulated by promoter methylation in prostate cancer cells. On the other hand, CTN06 downregulates Mir-421 (– 46.3 folds), which has been reported to downregulate ATM, a pro-apoptotic protein.⁴²

CTN06 downregulates oncogenic-related genes. To further explore the mechanism of anti-cancer effect of CTN06 in prostate cancer cells, cDNA microarray assay was performed in PC3 cells following treatment with CTN06. Among the 772 genes examined, 57 genes were down-regulated > 2 folds. Interestingly, 25 of which are oncogenic-related genes (Supplementary Figure S4c). Among those genes, Met, which is downregulated 2.1 folds following treatment with CTN06, has been reported to be constitutively activated in PC3 cells, and inhibition of Met led to significant inhibition of PC-3 cell proliferation, clonogenicity, migration and invasion.⁴⁴ MYCBP, which is downregulated 2.1 folds by CTN06, is a positive regulator of Myc. Downregulation of MYCBP by miR22 suppresses oncogenic Myc activity.⁴⁵

CTN06 has higher potency to inhibit prostate cancer cell growth compared with other kinase inhibitors. To further

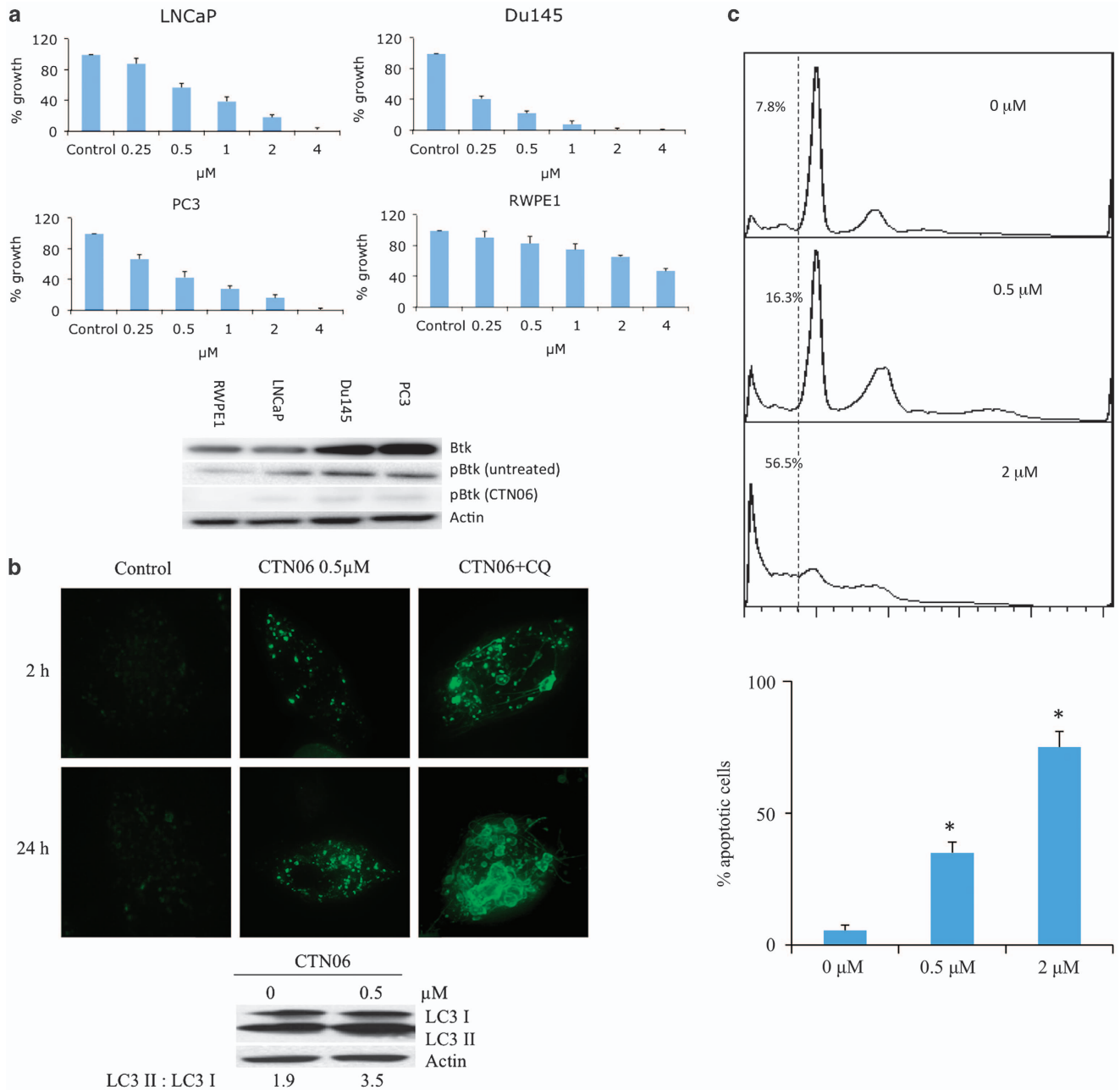


Figure 4 CTN06 induces autophagy as well as apoptosis in prostate cancer cells. **(a)** Growth inhibition of CTN06 to LNCaP, Du145, PC3 prostate cancer and normal prostate (RWPE1) cells. Cells were seeded at 5000 cells/well in 96-well plate overnight and treated with CTN06 at the indicated concentrations. The cell viability was measured using MTT assay after 72 h. Columns, mean; bars, standard deviation, $n = 3$. Inhibition of Btk by CTN06 ($0.5 \mu\text{M}$) in those cells was measured using western blot. **(b)** Induction of autophagy in PC3 cells by CTN06. PC3 cells were stably transfected with GFP-LC3 and were grown in 6-well plate to 50% confluence and treated with CTN06. Autophagy was visualized by GFP-LC3 'puncta' at 2 and 24 h and immunoblot of endogenous LC3 isoforms 24 h after treatment. **(c)** Induction of apoptosis of PC3 cells following treatment with CTN06. PC3 cells were seeded at 10^6 cells/ml (2 ml) in a 6-well plate overnight and then treated with CTN06 at the indicated concentrations for 24 h. Apoptosis was analyzed using PI staining as well as Annexin V-FITC apoptosis detection kit. Columns, mean; bars, standard deviation, $n = 3$. In all, 0.5 and $2 \mu\text{M}$ are significantly different from $0 \mu\text{M}$ (* $P < 0.05$, one-way ANOVA with Tukey test for pairwise comparison)

explore the potency of CTN06 to prostate cancer cells, growth inhibitory activity of CTN06 to PC3 cells was compared with other kinase inhibitors including saracatinib (AZD0530), sorafenib, AG1478, 3ATA and LMF-A13. At $2 \mu\text{M}$, CTN06 showed the highest potency to inhibit PC3 cell growth followed by sorafenib (Figure 6a). This result indicated that CTN06 is a potent inhibitor of prostate cancer cell growth.

CTN06 as a chemo-sensitizer. Our initial studies indicated that CTN06 has good cytotoxicity toward a panel of prostate cancer cells. To examine whether a Btk and Etk dual inhibitor works effectively as a chemo-sensitizer, PC3 cells were co-treated with CTN06 ($0.25 \mu\text{M}$) and the autophagy inhibitor CQ ($10 \mu\text{M}$), or docetaxel (DTX) (2 ng/ml). Growth inhibition was determined using an MTT assay after 72 h. Interestingly,

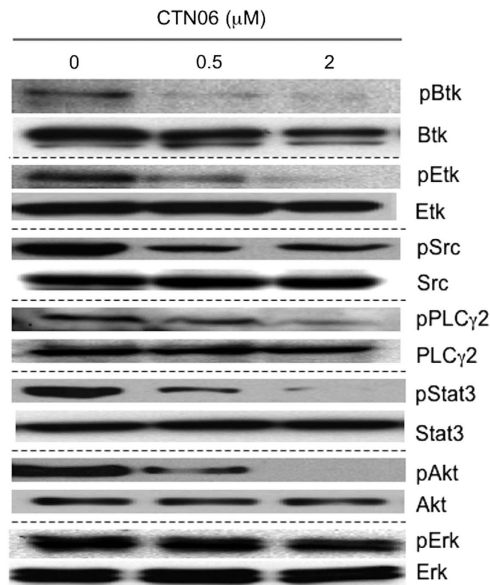


Figure 5 Inhibition of cell signaling in PC3 cells following treatment with CTN06. Cells were grown in 100-mm plate to 50% confluence and treated with CTN06 at the indicated concentrations. Cells were harvested after 12 h. pEtk, Etk, pBtk, Btk, pSrc, Src, pPLC γ 2, PLC γ 2, pStat3, Stat3, pAkt, Akt, pERK and ERK levels were measured using the corresponding antibodies by western blot. One of three similar experiments depicted

a synergistic effect of CTN06 was observed when prostate cancer cells were co-treated with CQ. In the case of DTX co-treatment, less of a synergistic effect was observed when CTN06 and DTX were added to the cells at the same time, while a striking synergistic effect was observed when cells were treated with DTX for 24 h before treatment with CTN06 (Figure 6b). Annexin-V and PI staining further confirmed that combination of CTN06 and CQ induced apoptosis (Figure 6c). This suggests that CTN06 is a chemo-sensitizer, and blocking of autophagy by CQ promotes CTN06-induced cell death.

CTN06 inhibits PC3 xenograft tumor growth *in vivo*. Given the *in vitro* activity of CTN06 against prostate cancer cells, it is important to validate these results *in vivo*. PC3 cells were injected subcutaneously to nude mice. The mice were treated with vehicle (control) or CTN06 at 10 mg/kg daily via IP injection. As shown in Figures 7a and b, CTN06 decreased PC3 xenograft tumor growth without significant toxicity. Furthermore, Ki67 staining indicated that CTN06 inhibited tumor growth activity and cleaved caspase 3 staining indicated that it also induced apoptosis (Figure 7c). Western blot of LC3I to LC3II conversion suggested autophagy induction in PC3 xenograft tumors by CTN06 (Figure 7d).

Discussion

Tyrosine kinases have become important targets for drug development. Powerful combinatorial chemistry approaches and high-throughput screening assays have led to successful identification of many kinase inhibitors.^{46–48} Our previous work indicated that Etk is complexed with Src and FAK, and

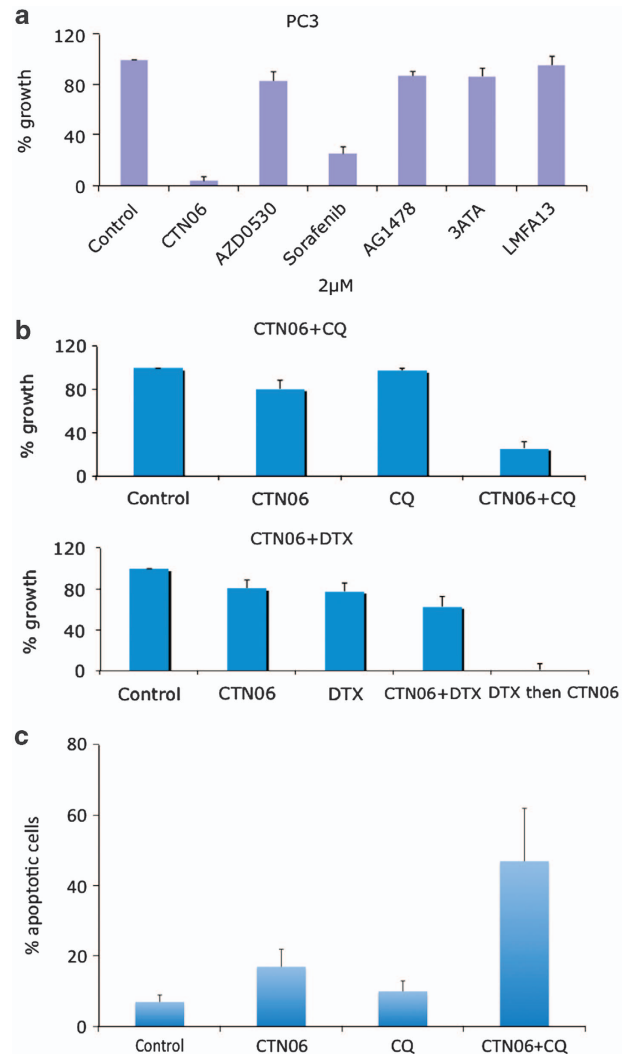


Figure 6 CTN06 as a chemo-sensitizer. (a) Comparison of CTN06 with other kinase inhibitors. PC3 cells were seeded at 5000 cells/well in 96-well plates overnight and treated with CTN06 or the other kinase inhibitors including AZD0530, sorafenib, AG1478, 3ATA and LMF-A13 at 2 μ M. The cell viability was measured using MTT assay after 72 h. (b) Growth inhibition of CTN06 and in combination with 10 μ M chloroquine (CQ) or 2 ng/ml docetaxel (DTX) to PC3 human prostate cancer cells. Cells were seeded at 5000 cells/well in 96-well plate overnight and pretreated with the corresponding co-treatments for 1 h, then treated with 0.25 μ M CTN06. The cell viability was measured using MTT assay after 72 h. (c) The apoptotic effect of CTN06 in combination with CQ to PC3 cells was further measured using Annexin-V and PI staining and flow cytometry. Columns, mean; bars, standard deviation, $n = 3$

has an important role in apoptosis, angiogenesis and metastasis of prostate cancer cells.²² Etk activation is a compensatory response to androgen deprivation, implicating its overexpression in castration-resistance transition.⁴⁹ In addition, Etk interacts with p53 and controls the apoptosis pathway.²⁵ Etk's role in other solid tumors including bladder cancer, hepatocellular carcinoma, nasopharyngeal carcinoma and breast cancer is well established.^{14–16,50} Etk has recently been implicated in the self-renewal and tumorigenic potential of glioblastoma stem cells.²⁶ Etk, highly expressed in endothelial cells, has been shown to be a critical tyrosine kinase for angiogenesis and tumor growth.¹⁸ All these findings

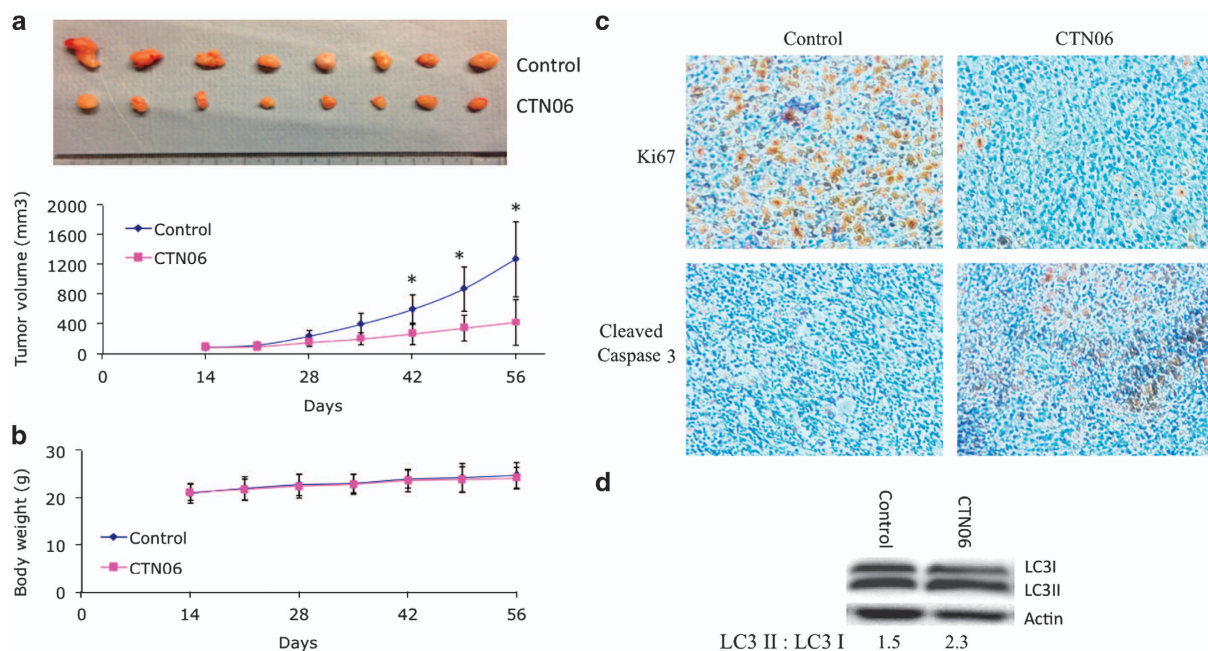


Figure 7 Inhibition of PC3 xenograft tumor growth by CTN06. 2×10^6 PC3 cells were injected subcutaneously to nude mice. The tumors were grown to the indicated size and the mice were randomly divided into two groups (8 mice/group). The control group was treated with vehicle. The treatment group was treated with CTN06 at 10 mg/kg daily via IP injection. (a and b) The tumor size and body weight were measured once a week. Marks, mean; bars, mean; $n = 8$ ($*P < 0.05$, one-way ANOVA with Tukey test for pairwise comparison). (c and d) The tumor samples were further analyzed for Ki67 and cleaved caspase 3 using immunohistochemistry and LC3I to LC3II conversion using western blot

point to Etk as an appropriate therapeutic target. Yet, surprisingly little is known about Etk selective inhibitors. One recent report showed that an EGFR inhibitor, CI-1033, inhibits Etk at a sub-micromolar level via irreversible modification of a conserved cysteine residue.⁵¹ In this study, we set forth to identify a selective inhibitor for Etk.

Perhaps, the most striking observation of this study is the discovery that not only Etk is involved in prostate carcinogenesis, but also its close relative Btk. Previously, Btk was mainly reported in B cells and B-cell malignancies. Btk inhibitors have been developed for the benefit of treating hematopoietic diseases. The role of Btk in solid tumors remains totally unknown. Here, we report that Btk is aberrantly expressed in prostate cancer tissues and cells. The Btk expression level increases with the higher grade tumors, and in the prostate cancer cell lines, it is expressed at a much higher level in androgen-independent cell lines than androgen-sensitive LNCaP cells or immortalized normal epithelial cells. Indeed, both Btk and Etk have a distinct but overlapping role in prostate cancer growth and survival. Knockdown of individual kinases attenuates the growth of PC3 cells, but simultaneous knockdown has greater effects. Thus, while we were screening for Etk inhibitors, we also look for those that inhibit both, and were able to identify CTN06 that inhibits both Etk and Btk and to a lesser extent, Itk. To our knowledge, this is the first selective Btk/Etk dual inhibitor reported to date.

CTN06 belongs to a novel class of reversible kinase inhibitors with a chemical structure distinct from other known TKIs. This inhibitor is most potent in inhibiting Btk followed by Etk. Compared with known Btk inhibitors, the inhibitory potency of CTN06 against Btk is about 100-fold stronger than LFM-A13 which is a reversible Btk inhibitor (Figure 3b). There

are few Etk inhibitors reported so far. CI-1033 is a potent irreversible EGFR inhibitor with moderate Etk inhibition, but clinical study reported that CI-1033 is associated with severe toxicity.⁵² Therefore, a reversible Etk inhibitor such as CTN06 may have advantages and is probably less toxic. Treatment of PC3 cells with CTN06 resulted in the decrease in phosphorylation of Btk and Etk, as well as the downstream signals PLC γ 2, Stat3 and Akt. Interestingly, Src phosphorylation was greatly inhibited in cells following treatment with CTN06 compared with kinase inhibition assay. This is likely due to inhibition of Etk, which has been shown to crossactivate Src.²¹ Significantly, CTN06 has much less effect on the growth of the immortalized normal prostate cell RWPE1, consistent with the Btk/Etk knockdown experimental results (Figure 2). While PC3 and DU145 have much higher expression level of Btk, LNCaP expresses both Etk and Btk about the same level as RWPE1; yet LNCaP appears to be more sensitive to CTN06 than RWPE1, suggesting that prostate cancer cells have adapted to the Etk/Btk pathway for growth and survival, much more so than normal prostate epithelial cells. This provides a strong rationale for targeting Btk/Etk pathway in prostate cancer cells. In addition, we and others previously reported that Src inhibitors such as saracatinib (AZD0530) or dasatinib, while effective in inhibiting metastasis, are generally not inducers of apoptosis, which is in part due to their ability to induce autophagy.^{30,53} By contrast, CTN-06 induces a high level of apoptosis, despite its ability to induce autophagy. This is likely due to the fact that Etk also interacts with and inactivates p53. Overexpression of Etk in prostate cancer cells is known to confer apoptosis resistance to androgen deprivation and photodynamic therapy.^{17,49} Given the anti-apoptotic role of Btk in B-cell malignancies, it is likely that

inhibition of Btk also contributes to the induction of apoptosis in prostate cancer cells. In addition, the effects of CTN06 on miRNAs could in part account for its ability to induce apoptosis in prostate cancer cells. This suggests that dual inhibitors of Btk/Etk, which connects to Src pathway, may offer a more effective alternative to Src inhibitors in terms of cell killing. Indeed, we found CTN06 is a much more effective growth inhibitor than AZD0530 (Figure 6a) as well as other currently approved anti-cancer drugs.

The finding that autophagy inhibitor CQ further enhances the apoptosis-inducing effect of CTN06 suggests that here, like that in the case of other tyrosine kinase inhibitors,³⁰ autophagy contributes partially to the survival of CTN06-treated cells. Thus, autophagy inhibitor may be considered to enhance the efficacy of this compound. CTN06 is also a chemo-sensitizer and showed synergistic effect with DTX, indicating its potential role in combination therapy for prostate cancer. Interestingly, the sequence of its application is important. DTX followed by CTN06 is more effective than the reverse. This is understandable, as DTX action requires the cell-cycle movement to G2/M phase, which may be impeded if CTN06 was added first. Finally, consistent with Etk's role in cellular movement and as a co-activator of FAK,²¹ CTN06 was found to inhibit migration of prostate cancer cells. We thus anticipate that CTN06 should also have the ability to limit tumor metastasis. However, the genetic characters (e.g., AR and p53 status) of prostate cancer may influence their responses to drug treatment. Further investigation is desired to explore the effect of these factors to the response of prostate cancer cells to CTN06.⁵⁴

In summary, we found that Btk is aberrantly expressed in prostate cancer, which together with Etk present suitable targets for therapy. We have identified a Btk and Etk dual inhibitor, CTN06, with good selectivity toward prostate cancer cells. Further evaluation of its pharmacokinetic and pharmacodynamic properties is underway. Btk and Etk dual inhibition holds exceptional promise as a novel treatment strategy for prostate cancer.

Materials and Methods

Reagents. Purified Etk, Btk, Itk, Mer, Yes, Lyn and Src kinases were obtained from Millipore Inc (Dundee, UK). PI, *N,N*-diisopropylethylamine (DIEA), *N,N*-dimethylformamide (DMF), ethanol, acetonitrile (ACN), *N*-Methyl-2-pyrrolidone (NMP), 1-(3-aminopropyl)piperidine, trifluoroacetic acid (TFA), Pd/C, ammonium formate, cyanogen bromide and dimethyl sulfoxide (DMSO) were purchased from Sigma-Aldrich (Saint Louis, MO, USA). L-Leucine methyl ester hydrochloride and 4-(4-pyridinyl)benzoic acid were purchased from Chem-Impex International Inc (Wood Dale, IL, USA). The Annexin V-FITC apoptosis detection kit was obtained from Abcam (Cambridge, MA, USA). Reverse-phase high-performance liquid chromatography (RP-HPLC) from the Waters Corporation (Milford, MA, USA) was used for analysis and purification of CTN06.

Synthesis of CTN06. In brief, a solution of L-leucine methyl ester hydrochloride (545.1 mg, 3.0 mmol) and DIEA (1.15 ml, 6.6 mmol) in DMF (4.5 ml) was added dropwise under vigorous stirring to a solution of 1,5-difluoro-2,4-dinitrobenzene (612.0 mg, 3.0 mmol) in DMF (1.5 ml). The reaction solution was stirred at room temperature for 45 min. This was followed by the addition of a solution of 1-(3-aminopropyl) piperidine (477 μ l, 3.0 mmol) and DIEA (522.6 μ l, 3.0 mmol) in DMF (2 ml). The resulting mixture was agitated at room temperature overnight. Ethanol (60 ml), Pd/C (10%, 600 mg) and ammonium formate (4.5 g, 71.4 mmol) were added to the solution. The solution was heated to reflux for 4 h and then cooled to room temperature. The Pd/C was filtered out and the filtrate

was concentrated with a rotary evaporator. The residue was re-dissolved in ethanol (40 ml), followed by addition of cyanogen bromide (321.3 mg, 3.6 mmol). The resulting mixture was stirred at room temperature for 12 h. The precipitate was collected by filtration and washed with ethanol, three times. The solid was dried in vacuum and used for the next step without further purification. A portion of the solid (382.5 mg, 1.0 mmol) was weighed out and re-dissolved in NMP (1 ml), and was added the solution of 4-(4-pyridinyl)benzoic acid (199.2 mg, 1.0 mmol), HBTU (379.3 mg, 1.0 mmol) and DIEA (348.4 μ l, 2.0 mmol) in NMP (3 ml). The resulting solution was stirred at room temperature overnight. The precipitate was collected by filtration and washed with ethanol followed by RP-HPLC purification. The fraction was collected and lyophilized to give a yellow powder as the final product (Supplementary Figure S1). The homogeneity of the compound was checked by analytical RP-HPLC. The purity was determined to be >95% pure. The identity of the compound was confirmed by matrix-assisted laser desorption/ionization-time of flight mass spectrometry, found: 564.28 Dalton (calculated: 564.31 Dalton for MH⁺).

Cell culture. RWPE1, LNCaP, Du145 and PC3 cells were obtained from ATCC (Manassas, VA, USA) and maintained in RPMI-1640 medium containing 10% fetal bovine serum and 1% penicillin/streptomycin/glutamine.

Tissue microarray. The expression level of Btk in prostate cancer tissue was examined using tissue microarray (PROS-006) from the UC Davis Pathology department. The array was stained with anti-Btk antibody (Santa Cruz Inc., Santa Cruz, CA, USA; sc-1107). The array contains 28 benign, 48 Gleason 6 (CaP 6), 46 Gleason 8 (CaP 8) prostate cancer samples. The expression level of Btk was graded as no, low and high as illustrated in Figure 1a by an expert pathologist.

Btk ELISA. Btk levels in RWPE1, LNCaP, Du145 and PC3 cells were further measured using the Btk ELISA assay kit (Abnova Inc., Littleton, CO, USA; KA2617) according to the manufacturer's protocol.

Reverse transcription and quantitative real-time PCR. Reverse transcription and quantitative real-time PCR (qRT-PCR) were done as described previously.³⁰ Primer sequences used to amplify Btk fragments are listed as follows: forward 5'-GGTGGAGAGCAGAGATAAA-3'; reverse 5'-CCGAGTCATG TGTTTGAATAC-3' (IDT DNA Inc., Coralville, IA, USA). GAPDH was used as the housekeeping gene.

Etk and Btk knockdown assay. Etk and Btk expression in PC3 and RWPE1 cells was knocked down using siRNA. The Btk (Smartpool), Etk (Smartpool) siRNA and non-targeted RNA were obtained from Dharmacon Inc. (Lafayette, CO, USA). The siRNAs were transfected to cells according to the manufacturer's instruction. The expression levels of Btk and Etk were examined using a western blot after 48 h. The growth rates were examined daily using an MTT assay for 3 days. For comparison of SiBtk and LFM-A13, PC3 and Du145 cells were seeded at 5000 cells/well in 96-well plate overnight. Then, the cells were transfected with SiBtk or treated with 50 μ M LFM-A13, cell viability was examined using an MTT assay at 72 h.

Kinase inhibition assay. Kinase inhibition was measured using TLC. Briefly, purified kinases (20 nM), the corresponding substrate (500 μ M, TSFYGRH for Etk, YIYGSFK for the other kinases) and CTN06 (0–10 μ M) were incubated in a kinase reaction (100 mM Hepes, pH 7.4, 10 mM MnCl₂, 10 mM MgCl₂, 1 mM DTT) for 5 min, and the reaction was started by adding 5 μ Ci ³³P-labeled ATP. The reaction (10 μ l) was incubated at room temperature for 1 h and was stopped by adding 10 μ l H₃PO₄. The radioactivity of the peptide substrate was analyzed using TLC as previously described.⁵⁵

Molecular modeling. Molecular docking studies were performed to determine the preferred binding site of CTN06 on the Btk structure. An energy optimized structure of CTN06 was calculated using Merck Molecular Force Field (MMFF) as implemented in Marvin Suite v 5.11 (<http://www.chemaxon.com/products/marvin>). The crystal structure of Btk (PDB ID: 1K2P) that corresponds to amino-acid positions 397–654 was used in our modeling studies. To define a putative binding site for CTN06 on Btk protein structure, we first used a blind docking approach, implemented on the SwissDock web service (<http://swissdock.vital-it.ch>).⁵⁶ Among the clusters generated by SwissDock, the conformation with the lowest binding free energy was selected. To further confirm the binding site predicted by blind docking, we used Autodock v4.2. Btk and

CTN06 structures were prepared for docking using an Autodock Tools package.⁵⁷ Partial atomic charges were assigned to CTN06 using the Gasteiger-Marsili method, and, after the merging of non-polar hydrogens, rotatable bonds were assigned using Autodock Tools. All the water molecules were removed from the Btk structure, and the missing hydrogens and Kollman partial charges were added. Further, non-polar hydrogens were merged to their corresponding carbons, and for each atom the desolvation parameters were assigned. We used a grid size of $60 \times 60 \times 60$ with grid spacing of 0.375 angstroms. The grid size was selected to fit the whole ligand molecule. We used the Lamarckian Genetic Algorithm, called Pseudo Solis-Wets Algorithm, to perform 256 independent docking runs with default parameters in Autodock.⁵⁸ Cluster analysis was performed on docked results using an RMS tolerance of 2 angstroms.

To further understand the stability and dynamics of the ligand-kinase complex, we performed a 20-ns molecular dynamics (MD) simulation, starting with the best-docked structure predicted by Autodock-independent runs. These simulations were performed using NAMD v 2.7b2.⁵⁹ CHARMM27 force fields were used to calculate the potentials of Btk, while CHARMM22 (as implemented in SwissParam, <http://swissparam.ch>)⁶⁰ force fields were used to calculate the potentials of CTN06. The kinase-ligand complex was solvated in a water box with periodic boundary conditions. Dimensions of the water box were selected to be at least 10 angstroms larger than the solute in every direction. The whole system was neutralized with 0.15 M NaCl. An initial minimization step was performed for 6000 steps, followed by 20 ns of relaxation. Trajectories of these simulations were visualized using VMD v 1.9 (<http://www.ks.uiuc.edu/Research/vmd/vmd-1.9/>) and the interactions between the kinase and the ligand were plotted using LigPlot+ v 1.4 and PyMol (<http://www.schrodinger.com/pymol/>).

Western blotting. Western blotting was performed as described previously.⁶¹ Cells were grown in 100 mm dishes to about 50% confluence and treated with vehicle (control) and CTN06 (0.5 and 2 μ M) for 12 h. Proteins were detected by the following antibodies: β -actin (Sigma-Aldrich, A1978), Btk (Santa Cruz Inc., sc-1107), pBtk (pY233, Abcam, ab68217), Etk (Santa Cruz Inc., sc8874), pEtk (pY40, 3211S), Src (2109), pSrc (pY416, 6943), PLC γ 2 (3872), pPLC γ 2 (pY759, 6943), Stat3 (12640), pStat3 (pY705, 4113), ERK (4696) and pERK (4695) were obtained from Cell Signaling Inc. (Beverly, MA, USA). For pBtk and pEtk, cells were pre-treated with 100 μ M pervanadate for 15 min before harvest.

MTT assay. Cells were seeded in 96-well plates and cultured overnight, followed by treatment with 0.1% DMSO, as a vehicle control, and CTN06 at the indicated concentrations for 72 h. Growth inhibition was measured using a 3-(4,5-Dimethylthiazol-2-yl)-2,5-diphenyltetrazolium bromide (MTT) assay (Roche Diagnostic, Mannheim, Germany) according to the manufacturer's protocol.

Flow cytometry. PC3 cells were treated with 0.1% DMSO (control) and CTN06 at the indicated concentrations for 24 h. Cell-cycle arrest was determined by the incorporation of propidium iodide (Sigma-Aldrich) into permeabilized cells. Cells undergoing apoptosis were identified using an Annexin V-FITC kit (Abcam), following the manufacturer's instructions. The cells were analyzed using a Coulter Epics XL flow cytometer (Beckman Coulter, Miami, FL, USA).

Microarray assay for miRNAs and cDNAs. PC3 cells were seeded at 10^5 cells/well in 6-well plate and treated with 0.5 μ M CTN06 for 18 h. Cells were harvested and RNA was isolated using a trizol reagent (Ambion Inc., Grand Island, NY, USA). Total RNA samples were submitted to the UC Davis Comprehensive Cancer Center's Genomics Shared Resource (GSR) for microarray profiling of gene and miRNA expression and subsequent data analysis. The methods are briefly described below.

Comprehensive gene expression profiling was performed with Affymetrix GeneChip Human Genome U133 Plus 2.0 (HG-U133 Plus 2.0) (Affymetrix Inc., Santa Clara, CA, USA) arrays according to standard protocols described by the manufacturer. Normalized probe set expression intensities were obtained using robust multi-array average (RMA) for probe summarization and normalization of background-adjusted and log-transformed perfect match probe intensity values. The data set was filtered to retain only those probe sets having expression values that exceeded the 5% lower cutoff threshold in at least one of the samples. Comparison analysis was then performed to identify genes that were differentially expressed between CTN06- and vehicle-treated cells. Criteria for the selection of genes exhibiting significant expression changes included an average fold change of ≥ 2.0 between groups and P -values of ≤ 0.05 . Global analysis of miRNA

expression was performed with Agilent Human miRNA Microarrays (Release 16.0) (Agilent Technologies, Santa Clara, CA, USA) as per the manufacturer's standard protocols. Background-subtracted signal intensity values were log-transformed, quantile-normalized and baseline transformed with GeneSpring GX12 software (Agilent Technologies). The data set was then filtered for miRNAs exhibiting ≥ 1.5 -fold differential expression in CTN06-treated cells relative to that of the vehicle-treated controls. The miRNA profile was examined using GeneChip miRNA 2.0 Array (Affymetrix Inc.) and the gene expression profile was examined using cDNA microarray (Affymetrix Inc.) by UC Davis Genome Center.

Autophagy assay. PC3 cells were stably transfected with GFP-LC3, as previously described.³⁰ Cells were grown in a 6-well plate to 50% confluence and treated with 5 μ M CTN06 for 24 h. Autophagy was visualized by GFP-LC3 'puncta' and immunoblot of Endogenous LC3 isoforms under an Olympus BX61 motorized reflected fluorescence microscope with FITC filter (excitation, 480 nm; emission, 535 nm) (Olympus America Inc., Melville, NY, USA) by using the SlideBook4.1 software (Intelligent Imaging Innovations, Denver, CO, USA).

PC3 cell 'wound healing' assay. PC3 cells were grown in 6-well plate to 60% confluency. Then wounds were made using a tip and treated with CTN06 (0 and 0.5 μ M). Cell migration (wound healing) was visualized under microscope at the indicated times.

CTN06 as a chemo-sensitizer. Growth inhibition of CTN06 in combination with 10 μ M CQ, 2 ng/ml DTX or 1 μ M AZD0530 (AZD), to PC3 human prostate cancer cells was evaluated. Cells were seeded at 5000 cells/well in a 96-well plate overnight and pre-treated with the corresponding co-treatments for 1 h, then treated with 0.25 μ M CTN06. The cell viability was measured using an MTT assay after 72 h.

Inhibition of PC3 xenograft tumor growth by CTN06. Animal experimental conditions were in accordance with the protocol approved by the Institutional Animal Care and Use Committee at the University of California, Davis. In all, 2×10^6 PC3 were injected subcutaneously to 5- to 6-week-old male nude mice. Mice were randomly divided into two groups and treated with buffer only (control) or 10 mg/kg/day CTN06 daily starting from 14 days after injection. The size of tumors and body weight were measured once a week. After 42 days treatment, mice were killed and tumors were harvested frozen in liquid nitrogen and stored at -80°C . Paraffin-embedded tumor tissues were sectioned to 5- μ m thickness and mounted on positively charged microscope slides, and 1 mM EDTA (pH 8.0) was used for antigen retrieval. Immunohistochemistry was performed using 1:200 dilution of Ki67 antibody (Cell Signaling Inc., 9027) and 1:50 dilution of cleaved caspase 3 antibody (Cell Signaling Inc., 9664). Western blots were performed using tumor lysates with LC3 antibody (Cell Signaling Inc., 4599).

Statistics. A one-way ANOVA was used in combination with a Tukey test for pairwise comparison. P -values of <0.05 were considered as significant.

Conflict of Interest

Both KSL and HJK are scientific advisors for C-TAG Inc.

Acknowledgements. This work was in part supported by C-TAG Bioscience Inc (Research grant to RL), NIH grants DOH102-TD-M-111-102001 (to HJK), NSC 102-2320-B-400-018-MY3 (to HJK), and 03A1-MGPP18-014 (to HJK), DK52659 CA150197 (to HJK) and CA098116 (to KSL); DOD Postdoctoral Training Award PC080859 and Auburn Community Cancer Endowment Fund (to WG); DOD Postdoctoral Training Award PC121738 (to GB); and a Stand Up to Cancer-Prostate Cancer Foundation Prostate Dream Team Translational Cancer Research Grant. This research grant is made possible by the generous support of the Movember Foundation. Stand Up To Cancer is a program of the Entertainment Industry Foundation administered by the American Association for Cancer Research.

1. Jemal A, Siegel R, Ward E, Hao Y, Xu J, Murray T et al. Cancer statistics 2008. *CA Cancer J Clin* 2008; **58**: 71-96.
2. Stommel JM, Kimmelman AC, Ying H, Nabioullin R, Ponugoti AH, Wiedemeyer R et al. Coactivation of receptor tyrosine kinases affects the response of tumor cells to targeted therapies. *Science* 2007; **318**: 287-290.

3. Honda F, Kano H, Kanegane H, Nonoyama S, Kim ES, Lee SK *et al*. The kinase Btk negatively regulates the production of reactive oxygen species and stimulation-induced apoptosis in human neutrophils. *Nat Immunol* 2012; **13**: 369–378.
4. Conley ME, Dobbs AK, Farmer DM, Kilic S, Paris K, Grigoriadou S *et al*. Primary B cell immunodeficiencies: comparisons and contrasts. *Annu Rev Immunol* 2009; **27**: 199–227.
5. Gray P, Dunne A, Brikos C, Jefferies CA, Doyle SL, O'Neill LA. MyD88 adapter-like (Mal) is phosphorylated by Bruton's tyrosine kinase during TLR2 and TLR4 signal transduction. *J Biol Chem* 2006; **281**: 10489–10495.
6. Khare A, Viswanathan B, Gund R, Jain N, Ravindran B, George A *et al*. Role of Bruton's tyrosine kinase in macrophage apoptosis. *Apoptosis* 2011; **16**: 334–346.
7. Herman SE, Gordon AL, Hertlein E, Ramanunni A, Zhang X, Jaglowski S *et al*. Bruton tyrosine kinase represents a promising therapeutic target for treatment of chronic lymphocytic leukemia and is effectively targeted by PCI-32765. *Blood* 2011; **117**: 6287–6296.
8. Rushworth SA, Bowles KM, Barrera LN, Murray MY, Zaitseva L, MacEwan DJ. BTK inhibitor ibrutinib is cytotoxic to myeloma and potently enhances bortezomib and lenalidomide activities through NF- κ B. *Cell Signal* 2013; **25**: 106–112.
9. Mahajan S, Ghosh S, Sudbeck EA, Zheng Y, Downs S, Hupke M *et al*. Rational design and synthesis of a novel anti-leukemic agent targeting Bruton's tyrosine kinase (BTK), LFM-A13 [alpha-cyano-beta-hydroxy-beta-methyl-N-(2, 5-dibromophenyl)propenamide]. *J Biol Chem* 1999; **274**: 9587–9599.
10. de Rooij MF, Kuil A, Geest CR, Eldering E, Chang BY, Buggy JJ *et al*. The clinically active BTK inhibitor PCI-32765 targets B-cell receptor- and chemokine-controlled adhesion and migration in chronic lymphocytic leukemia. *Blood* 2012; **119**: 2590–2594.
11. Winer ES, Ingham RR, Castillo JJ. PCI-32765: a novel Bruton's tyrosine kinase inhibitor for the treatment of lymphoid malignancies. *Expert Opin Investig Drugs* 2012; **21**: 355–361.
12. Chang BY, Huang MM, Francesco M, Chen J, Sokolove J, Magadala P *et al*. The Bruton tyrosine kinase inhibitor PCI-32765 ameliorates autoimmune arthritis by inhibition of multiple effector cells. *Arthritis Res Ther* 2011; **13**: R115.
13. Tai YT, Chang BY, Kong SY, Fulciniti M, Yang G, Calle Y *et al*. Bruton tyrosine kinase inhibition is a novel therapeutic strategy targeting tumor in the bone marrow microenvironment in multiple myeloma. *Blood* 2012; **120**: 1877–1887.
14. Guo S, Sun F, Guo Z, Li W, Alfano A, Chen H, Magyar CE *et al*. Tyrosine kinase ETK/BMX is up-regulated in bladder cancer and predicts poor prognosis in patients with cystectomy. *PLoS One* 2011; **6**: e17778.
15. Zhang Z, Zhu W, Zhang J, Guo L. Tyrosine kinase Etk/BMX protects nasopharyngeal carcinoma cells from apoptosis induced by radiation. *Cancer Biol Ther* 2011; **11**: 690–698.
16. Guo L, Guo Y, Xiao S. Expression of tyrosine kinase Etk/Bmx and its relationship with AP-1- and NF-kappaB-associated proteins in hepatocellular carcinoma. *Oncology* 2007; **72**: 410–416.
17. Xue LY, Qiu Y, He J, Kung HJ, Oleinick NL. Etk/Bmx, a PH-domain containing tyrosine kinase, protects prostate cancer cells from apoptosis induced by photodynamic therapy or thapsigargin. *Oncogene* 1999; **18**: 3391–3398.
18. Chang YM, Kung HJ, Evans CP. Nonreceptor tyrosine kinases in prostate cancer. *Neoplasia* 2007; **9**: 90–100.
19. Dai B, Kim O, Xie Y, Guo Z, Xu K, Wang B *et al*. Tyrosine kinase Etk/BMX is up-regulated in human prostate cancer and its overexpression induces prostate intraepithelial neoplasia in mouse. *Cancer Res* 2006; **66**: 8058–8064.
20. Holopainen T, López-Alpuche V, Zheng W, Hellasvaara R, Jones D, He Y *et al*. Deletion of the endothelial Bmx tyrosine kinase decreases tumor angiogenesis and growth. *Cancer Res* 2012; **72**: 3512–3521.
21. Lee LF, Guan J, Qiu Y, Kung HJ. Neuropeptide-induced androgen independence in prostate cancer cells: roles of nonreceptor tyrosine kinases Etk/Bmx, Src, and focal adhesion kinase. *Mol Cell Biol* 2001; **21**: 8385–8397.
22. Chen R, Kim O, Li M, Xiong X, Guan JL, Kung HJ *et al*. Regulation of the PH-domain-containing tyrosine kinase Etk by focal adhesion kinase through the FERM domain. *Nat Cell Biol* 2001; **3**: 439–444.
23. Jiang X, Borgesi RA, McKnight NC, Kaur R, Carpenter CL, Balk SP. Activation of nonreceptor tyrosine kinase Bmx/Etk mediated by phosphoinositide 3-kinase, epidermal growth factor receptor, and ErbB3 in prostate cancer cells. *J Biol Chem* 2007; **282**: 32689–32698.
24. Qiu Y, Robinson D, Pretlow TG, Kung HJ. Etk/Bmx, a tyrosine kinase with a pleckstrin-homology domain, is an effector of phosphatidylinositol 3'-kinase and is involved in interleukin 6-induced neuroendocrine differentiation of prostate cancer cells. *Proc Natl Acad Sci USA* 1998; **95**: 3644–3649.
25. Jiang T, Guo Z, Dai B, Kang M, Ann DK, Kung HJ *et al*. Bi-directional regulation between tyrosine kinase Etk/BMX and tumor suppressor p53 in response to DNA damage. *J Biol Chem* 2004; **279**: 50181–50189.
26. Guryanova OA, Wu Q, Cheng L, Lathia JD, Huang Z, Yang J *et al*. Nonreceptor tyrosine kinase BMX maintains self-renewal and tumorigenic potential of glioblastoma stem cells by activating STAT3. *Cancer Cell* 2011; **19**: 498–511.
27. Chau CH, Chen KY, Deng HT, Kim KJ, Hosoya K, Terasaki T *et al*. Coordinating Etk/Bmx activation and VEGF upregulation to promote cell survival and proliferation. *Oncogene* 2002; **21**: 8817–8829.
28. Lou Y, Owens TD, Kuglstatler A, Kondru RK, Goldstein DM. Bruton's tyrosine kinase inhibitors: approaches to potent and selective inhibition, preclinical and clinical evaluation for inflammatory diseases and B cell malignancies. *J Med Chem* 2012; **55**: 4539–4550.
29. Kuglstatler A, Wong A, Tsing S, Lee SW, Lou Y, Villaseñor AG *et al*. Insights into the conformational flexibility of Bruton's tyrosine kinase from multiple ligand complex structures. *Protein Sci* 2011; **20**: 428–436.
30. Wu Z, Chang PC, Yang JC, Chu CY, Wang LY, Chen NT *et al*. Autophagy blockade sensitizes prostate cancer cells towards Src family kinase inhibitors. *Genes Cancer* 2010; **1**: 40–49.
31. Tsai YT, Su YH, Fang SS, Huang TN, Qiu Y, Jou YS *et al*. Etk, a Btk family tyrosine kinase, mediates cellular transformation by linking Src to STAT3 activation. *Mol Cell Biol* 2000; **20**: 2043–2054.
32. Wang XY, Wu MH, Liu F, Li Y, Li N, Li GY *et al*. Differential miRNA expression and their target genes between NGX6-positive and negative colon cancer cells. *Mol Cell Biochem* 2010; **345**: 283–290.
33. Gattolliat CH, Thomas L, Ciafrè SA, Meurice G, Le Teuff G, Job B *et al*. Expression of miR-487b and miR-410 encoded by 14q32.31 locus is a prognostic marker in neuroblastoma. *Br J Cancer* 2011; **105**: 1352–1361.
34. Zhang S, Hao J, Xie F, Hu X, Liu C, Tong J *et al*. Downregulation of miR-132 by promoter methylation contributes to pancreatic cancer development. *Carcinogenesis* 2011; **32**: 1183–1189.
35. Formosa A, Lena AM, Markert EK, Cortelli S, Miano R, Mauriello A *et al*. DNA methylation silences miR-132 in prostate cancer. *Oncogene* 2013; **32**: 127–134.
36. Navarro A, Diaz T, Martinez A, Gaya A, Pons A, Gel B *et al*. Regulation of JAK2 by miR-135a: prognostic impact in classic Hodgkin lymphoma. *Blood* 2009; **114**: 2945–2951.
37. Wang WL, Chatterjee N, Chittur SV, Welsh J, Tenniswood MP. Effects of 1 α ,25 dihydroxyvitamin D3 and testosterone on miRNA and mRNA expression in LNCaP cells. *Mol Cancer* 2011; **10**: 58.
38. Zhang Y, Liao JM, Zeng SX, Lu H. p53 downregulates Down syndrome-associated DYRK1A through miR-1246. *EMBO Rep* 2011; **12**: 811–817.
39. Kim WK, Park M, Kim YK, Tae YK, Yang HK, Lee JM *et al*. MicroRNA-494 downregulates KIT and inhibits gastrointestinal stromal tumor cell proliferation. *Clin Cancer Res* 2011; **17**: 7584–7594.
40. Ghisi M, Corradin A, Basso K, Frasson C, Serafin V, Mukherjee S *et al*. Modulation of microRNA expression in human T-cell development: targeting of NOTCH3 by miR-150. *Blood* 2011; **117**: 7053–7062.
41. Wang B, Li W, Guo K, Xiao Y, Wang Y, Fan J. miR-181b promotes hepatic stellate cells proliferation by targeting p27 and is elevated in the serum of cirrhosis patients. *Biochem Biophys Res Commun* 2012; **421**: 4–8.
42. Hu H, Du L, Nagabayashi G, Seeger RC, Gatti RA. ATM is down-regulated by N-Myc-regulated microRNA-421. *Proc Natl Acad Sci USA* 2010; **107**: 1506–1511.
43. Zhang Y, Gong W, Dai S, Huang G, Shen X, Gao M *et al*. Downregulation of human farnesoid X receptor by miR-421 promotes proliferation and migration of hepatocellular carcinoma cells. *Mol Cancer Res* 2012; **10**: 516–522.
44. Dai Y, Siemann DW. Constitutively active c-Met kinase in PC-3 cells is autocrine-independent and can be blocked by the Met kinase inhibitor BMS-777607. *BMC Cancer* 2012; **12**: 1–98.
45. Xiong J, Du Q, Liang Z. Tumor-suppressive microRNA-22 inhibits the transcription of E-box-containing c-Myc target genes by silencing c-Myc binding protein. *Oncogene* 2010; **29**: 4980–4988.
46. Lam KS, Salmon SE, Hersh EM, Hruby VJ, Kazmierski WM, Knapp RJ. A new type of synthetic peptide library for identifying ligand-binding activity. *Nature* 1991; **354**: 82–84.
47. McDonald OB, Chen WJ, Ellis B, Hoffman C, Overton L, Rink M *et al*. A scintillation proximity assay for the Raf/MEK/ERK kinase cascade: high-throughput screening and identification of selective enzyme inhibitors. *Anal Biochem* 1999; **268**: 318–329.
48. Wilhelm S, Carter C, Lynch M, Lowinger T, Dumas J, Smith RA *et al*. Discovery and development of sorafenib: a multikinase inhibitor for treating cancer. *Nat Rev Drug Discov* 2006; **5**: 835–844.
49. Dai B, Chen H, Guo S, Yang X, Linn DE, Sun F *et al*. Compensatory upregulation of tyrosine kinase Etk/BMX in response to androgen deprivation promotes castration-resistant growth of prostate cancer cells. *Cancer Res* 2010; **70**: 5587–5596.
50. Bagheri-Yarmand R, Mandal M, Taludker AH, Wang RA, Vadlamudi RK, Kung HJ *et al*. Etk/Bmx tyrosine kinase activates Pak1 and regulates tumorigenicity of breast cancer cells. *J Biol Chem* 2001; **276**: 29403–29409.
51. Hur W, Velentza A, Kim S, Flatauer L, Jiang X, Valente D *et al*. Clinical stage EGFR inhibitors irreversibly alkylate Bmx kinase. *Bioorg Med Chem Lett* 2008; **18**: 5916–5919.
52. Campos S, Hamid O, Seiden MV, Oza A, Plante M, Potkul RK *et al*. Multicenter, randomized phase II trial of oral CI-1033 for previously treated advanced ovarian cancer. *J Clin Oncol* 2005; **23**: 5597–5604.
53. Yang JC, Bai L, Yap S, Gao AC, Kung HJ, Evans CP. Effect of the specific Src family kinase inhibitor saracatinib on osteolytic lesions using the PC-3 bone model. *Mol Cancer Ther* 2010; **9**: 1629–1637.

54. van Bokhoven A, Varella-Garcia M, Korch C, Johannes WU, Smith EE, Miller HL *et al*. Molecular characterization of human prostate carcinoma cell lines. *Prostate* 2003; **57**: 205–225.
55. Lou Q, Wu J, Lam KS. A protein kinase assay system for both acidic and basic peptides. *Anal Biochem* 1996; **235**: 107–109.
56. Grosdidier A, Zoete V, Michielin O, Swiss Dock. a protein-small molecule docking web service based on EADock DSS. *Nucleic Acids Res* 2011; **39**: W270–W277.
57. Morris GM, Huey R, Lindstrom W, Sanner MF, Belew RK, Goodsell DS *et al*. AutoDock4 and AutoDockTools4: automated docking with selective receptor flexibility. *J Comput Chem* 2009; **30**: 2785–2791.
58. Solis FJ, Wets RJB. Minimization by random search techniques. *Math Oper Res* 1981; **6**: 19–30.
59. Phillips JC, Braun R, Wang W, Gumbart J, Tajkhorshid E, Villa E *et al*. Scalable molecular dynamics with NAMD. *J Comput Chem* 2005; **26**: 1781–1802.
60. Zoete V, Cuendet MA, Grosdidier A, Michielin O. SwissParam: a fast force field generation tool for small organic molecules. *J Comput Chem* 2011; **32**: 2359–2368.
61. Grasso AW, Wen D, Miller CM, Rhim JS, Pretlow TG, Kung HJ. ErbB kinases and NDF signaling in human prostate cancer cells. *Oncogene* 1997; **15**: 2705–2716.



Cell Death and Disease is an open-access journal published by **Nature Publishing Group**. This work is licensed under a **Creative Commons Attribution-NonCommercial-ShareAlike 3.0 Unported License**. The images or other third party material in this article are included in the article's Creative Commons license, unless indicated otherwise in the credit line; if the material is not included under the Creative Commons license, users will need to obtain permission from the license holder to reproduce the material. To view a copy of this license, visit <http://creativecommons.org/licenses/by-nc-sa/3.0/>

Supplementary Information accompanies this paper on Cell Death and Disease website (<http://www.nature.com/cddis>)